Sluggish Hadean geodynamics: Evidence from coupled 146,147 Sm– 142,143 Nd systematics in Eoarchean supracrustal rocks of the Inukjuak domain (Québec)

G. Caro, P. Morino, S.J. Mojzsis, N.L. Cates, W. Bleeker

Sluggish Hadean geodynamics: Evidence from coupled ^{146,147}Sm-^{142,143}Nd systematics in Eoarchean supracrustal rocks of the Inukjuak domain (Québec)

G. Caro[1,2] (corresponding author), P. Morino[1], S. J. Mojzsis[2,3], N. L. Cates[2], W. Bleeker[4]

[1] Centre de Recherches Pétrographiques et Géochimiques (CRPG), UMR 7358, Université de Lorraine, CNRS, 54500 Vandœuvre-lès-Nancy, France. caro@crpg.cnrs-nancy.fr

[2] Collaborative for Research in Origins (CRiO), Department of Geological Sciences, University of Colorado, UCB 399, 2200 Colorado Avenue, Boulder, CO 80309-0399, USA

[3] Institute for Geological and Geochemical Research, Research Center for Astronomy and Earth Sciences, Hungarian Academy of Sciences, 45 Budaörsi Street, H-1112 Budapest, Hungary

[4] Geological Survey of Canada, Natural Resources Canada, 601 Booth Street, Ottawa, ON K1S 0E8, Canada

Abstract: 366 words

Main Text: 6840 words

10 figures

1 Table

1 Appendix (electronic supplement)

Keywords: ^{146}Sm-^{142}Nd, Hadean, magma ocean, sluggish tectonics, Ukaliq, Nuvvuagittuq.

Abstract

The discovery of deficits in $^{142}Nd/^{144}Nd$ in mafic rocks of the Nuvvuagittuq Supracrustal Belt (NSB) has triggered a debate about the possible preservation of Hadean (pre-3.85 Ga) crustal remnants in the little-known but areally extensive Innuksuac complex (3.6-3.8 Ga, Inukjuak domain, Northeast Superior Province, Canada). Geochronological investigations in the NSB, however, are hampered by the poor preservation and highly disturbed isotopic record of various mafic (amphibolite) lithologies that host the ^{142}Nd anomalies. Here we present ^{146}Sm-^{142}Nd and ^{147}Sm-^{143}Nd data for rocks of extrusive magmatic and sedimentary protoliths from the Ukaliq supracrustal belt, a newly discovered volcano-sedimentary enclave locked within granitoid gneisses of the Inukjuak domain. Our study also includes the first ^{146}Sm-^{142}Nd data for quartz-magnetite rocks (banded iron-formation; BIF) of the NSB and the Eoarchean Isua supracrustal belt (ISB) in southern West Greenland. We show that Ukaliq amphibolites carry variably negative ^{142}Nd anomalies, ranging from 0 to -10 ppm, which are positively correlated with their Sm/Nd ratio. If considered as an isochron relationship, the ^{146}Sm-^{142}Nd array yields an apparent Hadean emplacement age of 4215^{+50}_{-76} Ma*. The negative ^{142}Nd anomalies, however, appear to be mainly restricted to amphibolites with boninitic affinities, likely reflecting inheritance from an enriched mantle source. In contrast, tholeiitic and ultramafic lavas have normal $\mu^{142}Nd$ regardless of their Sm/Nd ratio. Furthermore, BIF from Ukaliq and Nuvvuagittuq lack the negative ^{142}Nd anomalies that should have been produced by in situ decay of ^{146}Sm had these sediments been deposited prior to ca. 4.1 Ga. Instead, they exhibit $\mu^{142}Nd$ identical to that measured in Isua BIF. Collectively, our results suggest that the ^{146}Sm-^{142}Nd array characterizing mafic lithologies of Ukaliq and Nuvvuagittuq is an inherited signature with doubtful chronological significance. We interpret the volcanic protoliths of the Innuksuac complex to have been produced by metasomatically triggered melting of a variably enriched Eoarchean mantle, following addition of felsic melts and/or fluids derived from a foundering Hadean mafic crust. Application of coupled $^{146,147}Sm$-$^{142,143}Nd$ chronometry to Ukaliq lavas yields a model age of differentiation of* $4.36^{+0.05}_{-0.06}$ *Ga for this Hadean*

precursor. This is similar to late-stage crystallization ages inferred for the lunar and terrestrial magma oceans. The long-term preservation of Earth's primordial crust points to subdued lithospheric recycling in the post-magma ocean Earth.

1. Introduction

In the absence of an actual rock record of the first 500 Myr of Earth's history – as opposed to detrital Hadean zircons separated from their parent rocks (e.g. Mojzsis et al., 2001) – direct constraints on the composition, dynamics, and ultimate fate of the primordial lithosphere remain out of reach. Alternatively, indirect studies of the daughter products of short-lived radioactive nuclides show that the silicate Earth experienced early (4.4-4.5 Ga) differentiation (Harper and Jacobsen, 1992; Bennett et al., 2007; Boyet, 2005; Boyet et al., 2003; Caro et al., 2003), most likely due to the crystallization of a deep magma ocean in the aftermath of the moon-forming giant impact. By analogy to the lunar magma ocean model, it has been suggested that Earth's primordial crust was produced via upward migration and crystallization of mafic/ultramafic residual liquids in the final stages of solidification of the uppermost mantle (Caro et al., 2005; Bourdon and Caro, 2007; Rizo et al., 2011). Whereas various chronological aspects of these early events continue to be refined, the fate of Earth's primordial silicate reservoirs and the extent to which magma ocean processes subsequently influenced the geodynamic evolution of our planet, is enigmatic. Geochemical and isotopic studies of Jack Hills zircons suggest that magma ocean crystallization was rapidly followed by the onset of crustal formation processes akin to those operating in the modern Earth (e.g. Harrison, 2009). Precious little is known beyond this, however, about the geodynamic processes by which the primordial lithosphere was returned to the mantle, or the timescale associated with it.

The question of the rise (and demise) of the terrestrial protocrust is intrinsically connected to that of the geodynamic regime prevailing in the Hadean. A common view, based mostly on petrological and structural arguments, is that subduction (*sensu stricto*) was inoperative until the late Archean (Shirey

and Richardson, 2011; Bédard et al., 2003) and that renewal of the Earth's crust before that time operated in a “vertical tectonic” regime (Robin and Bailey, 2009). This view is supported by thermal evolution models which predict that in the hot early Earth mantle melting would have taken place at greater depth than today, generating a thicker crust associated with a highly depleted lithospheric mantle (Johnson et al., 2013; Korenaga, 2006; Vlaar et al., 1994; Sleep and Windley, 1982). Consequently, the Hadean lithosphere was likely stiffer and more buoyant, inhibiting the development of subduction zones and favoring instead a sluggish tectonic style characterized by slower plate motion and an overall longer crustal residence time (Korenaga, 2006; Foley et al., 2014). Alternatively, hotter mantle temperatures may have pushed the young Earth into a stagnant-lid regime (O’Neill and Debaille, 2014), where the mantle is overlain by a mechanically strong and generally immobile lithosphere, and crustal recycling only takes place during episodic pulses of rapid subduction. Lastly, gravitational instabilities in the thickened Hadean crust may have caused catastrophic episodes of rapid foundering and rejuvenation of the entire lithosphere (van Thienen et al., 2004).

The main obstacle to distinguishing these very different scenarios is the paucity of reworked Hadean components in the Archean rock record. In this context, the presence of deficits in $^{142}Nd/^{144}Nd$ in magmatic rocks of the Nuvvuagittuq supracrustal belt (NSB), within the Archean Innuksuac gneiss complex (Northeastern Superior province, Quebec), has major implications for our understanding of Hadean geodynamics (O’Neil et al., 2008; Roth et al., 2013). Due to the short half-life of ^{146}Sm ($T_{1/2}$=103 Myr), ^{142}Nd heterogeneities can only have been produced prior to about 4.1 Ga, and, therefore, are specifically related to mantle-crust differentiation in the Hadean (e.g. Caro, 2011). As Nd is more incompatible than Sm, enriched silicate reservoirs such as Earth’s Hadean crust would be characterized by relatively low Sm/Nd ratios, resulting in the development of negative ^{142}Nd anomalies (low $^{142}Nd/^{144}Nd$), whereas the complementary depleted mantle would develop positive ^{142}Nd anomalies. The ubiquitous presence of negative ^{142}Nd anomalies in mafic lithologies of the NSB has thus raised the question of whether actual Hadean volcano-sedimentary sequences are

preserved in the Inukjuak domain, or if this terrane instead inherited the geochemical fingerprint of a long vanished Hadean reservoir (O'Neil et al., 2008; Roth et al., 2013; Guitreau et al., 2014).

Innate negative ^{142}Nd anomalies from reworked Hadean components have also been reported from granitoids and mafic rocks of the Acasta gneisses (3.96 Ga, Slave craton, Canada (Mojzsis et al., 2014; Roth et al., 2014), the Schapenburg komatiite (Puchtel et al., 2016) and some 3.4 Ga Ameralik dykes of Southwest Greenland (Rizo et al., 2012). Likewise, the negative ^{142}Nd anomalies carried by Eoarchean tonalite-trondhjemite-granodiorite (TTG) rocks associated with the NSB (i.e. the Voizel suite) provide clear evidence for a variable degree of geochemical inheritance in plutonic rocks of the Innuksuac complex (O'Neil et al., 2008; Roth et al., 2013). At odds with this interpretation, O'Neil et al. (2008) proposed that the NSB still contains vestiges of the Hadean precursor in which the ^{142}Nd effect was produced, present as a heterogeneous package of highly altered mafic rocks (cummingtonite-rich amphibolite) colloquially termed by them the "Ujaraaluk unit" (O'Neil et al., 2011). This interpretation relies on the argument that NSB cummingtonite-amphibolites exhibit ^{142}Nd/^{144}Nd signatures that positively correlate with their Sm/Nd ratio (O'Neil et al., 2008). This characteristic was observed neither in the Acasta, Schapenburg, or Ameralik rocks cited above, and as such could be taken to represent a disturbed yet geochronologically significant isochron relationship. If the interpretation of O'Neil and co-workers is correct, then the volcano-sedimentary sequence of the NSB would represent the oldest preserved crust on Earth, and accordingly its geochemical record would have the potential to constrain the geodynamic and environmental state of our planet to within less than 300 Myr after the Moon-forming event.

Yet, the interpretation of the ^{146}Sm-^{142}Nd signal as a true isochron in the NSB rocks is not without caveats. First, the chronological constraints provided by the ^{147}Sm-^{143}Nd and ^{146}Sm-^{142}Nd chronometers are in fact strongly discordant; the cummingtonite-amphibolites define a younger ^{147}Sm-^{143}Nd errochron at ca. 3.6 Ga (O'Neil et al., 2012), and the apparent decoupling of the two Sm-Nd chronometers is not well understood (O'Neil et al., 2012; Roth et al., 2013). Second, quartz-biotite

schists and quartzites of probable detrital origin from the NSB show robust detrital zircon populations in a 3.65-3.78 Ga range, inconsistent with deposition in the Hadean (David et al., 2006; Cates and Mojzsis, 2007; Cates et al., 2013; Darling et al., 2013). Cates and Mojzsis (2007) also established a firm minimum age for the sequence at 3.75 Ga from a trondhjemitic sheet crosscutting amphibolites and BIF near the southern tip of the belt. The geochronological implications of these results depend on the nature of zircon-bearing protoliths, as well as their field relationship with the cummingtonite-amphibolite unit, the contentious nature of which has produced diverging interpretations of the zircon record (Augland and David, 2015; Darling et al., 2013). Nevertheless, the picture that emerges from conventional geochronological approaches points towards an Eoarchean age for the NSB, in contrast to the ca. 4.3 Ga date provided by the ^{146}Sm-^{142}Nd system. Hence, while the isotopic signal carried by Nuvvuagittuq rocks is exceptional – and may hold the key to a better understanding of the Hadean geological evolution – the fundamentals of both its chronological and geodynamic significance remain unclear.

The geochronological issue raised by the NSB ^{146}Sm-^{142}Nd record is further exacerbated by the poor preservation of the mafic lithologies carrying the ^{142}Nd anomalies (O'Neil et al., 2011). This is due to hydrothermal and metamorphic processes (e.g. Cates and Mojzsis, 2009) which resulted in severe disturbance of their geochemical signatures and currently prevents reliable dating using conventional radiogenic isotope systems (Guitreau et al., 2013; O'Neil et al., 2012; Roth et al., 2013; Touboul et al., 2014). The Nuvvuagittuq belt, however, is not the singular occurrence of supracrustal rocks in the wider Innuksuac complex; regional mapping, aerial photographs and aeromagnetic surveys also show the presence of a dozen or so scattered supracrustal enclaves in the general area of the Inukjuak domain (Simard et al., 2003), none of which have previously been subject to any detailed field or geochronological investigation. Here, we present high-precision ^{146,147}Sm-^{142,143}Nd data for a mapped unit of magmatic and sedimentary rocks from the Ukaliq[1] supracrustal belt (USB), a newly discovered

[1] Ukaliq (ᐅᑲᓕᖅ) is « Arctic hare » *Lepus arcticus* in the local *Inuktitut* language of Nunavik in northern Québec, and is used by us as an informal field name for this supracrustal enclave.

volcano-sedimentary enclave situated a few kilometers north of the NSB. Our results show that mafic lithologies of the USB define a rough positive correlation between $^{142}Nd/^{144}Nd$ and Sm/Nd, which, if interpreted as an isochron, would yield a Hadean emplacement age similar to that reported for Nuvvuagittuq. Our observations, however, consistently point towards an inherited origin for the ^{142}Nd effects. We show how this vestigial signal in turn provides a means to better understand the geodynamic evolution of the young Earth, from the crystallization of the magma ocean to the genesis of the oldest continental nuclei.

2. Geological setting

The Ukaliq supracrustal belt (USB) belongs to one of several scattered enclaves of the Innuksuac complex, a group of plutonic and supracrustal rocks rafted within the predominantly Neoarchean Inukjuak domain (Minto block, Northeast Superior Province (NESP), Quebec). The geology of the region has been described in detail in several previous studies (e.g. Cates and Mojzsis, 2007, 2009, 2013; Stevenson et al., 2006; O'Neil et al., 2007) and we only focus here on the newly discovered Ukaliq outcrops. The Ukaliq enclave (Fig. 1) is composed of interleaved rocks of volcanic and sedimentary protolith that are intruded by late leucogranitoids and surrounded by 3.45-3.65 Ga old tonalitic gneisses of the Voizel suite. Located approximately 5-10 km north of Nuvvuagittuq, the USB is an asymmetrical belt with a maximum thickness of 60 m and a NNW extent of several kilometers. Its southernmost exposure – the focus of this study – is within a low-strain window dominated by amphibolites (*Am*) and variably serpentinized ultramafic rocks (*Aum*), with minor sedimentary components including Iron formations (*BIF*), quartzite (*Aq*) and quartz-biotite shists (*Aqbc*) of probable detrital sedimentary origin. Although the Ukaliq enclave is intact, the sequence has been strongly deformed, transposed, and like the rest of the Inukjuak domain was metamorphosed to the upper amphibolite facies (Cates and Mojzsis, 2009). The ultramafic units show clear evidence at the outcrop for extensive alteration, and range from pure serpentinites on the eastern side of the

sequence to more pyroxene-rich compositions toward the West. We interpret this field relation to reflect a relict magmatic differentiation trend within a komatiitic flow. The presence of chemical sediments near to what we interpret to be the base of the sequence points to a predominantly volcanic or subvolcanic origin for the mafic/ultramafic rocks. It is noteworthy that unlike in the NSB, cummingtonite-rich amphibolites rarely occur in the USB. We interpret this to reflect the absence of the hydrothermally altered, low-Ca mafic lithologies that volumetrically dominate in the Nuvvuagittuq belt.

Our sample set was collected in the mapped exposures on the southern part of the USB during fieldwork in 2012 and 2014. The collection consists of 38 amphibolites and ultramafic rocks, 6 chemical sediments, 13 granitoid gneisses (Voizel suite), and 2 Neoarchean granites (Boizard suite) sampled from the enclosing gneisses of the supracrustals. Sample locations are reported on the map (Fig. 1), and correlated GPS coordinates are provided in Appendix A1.

3. Whole-rock geochemistry

3.1. Mafic and ultramafic rocks

Whole-rock major and trace element analyses were performed on amphibolites and ultramafic rocks representative of the main lithological units of the USB (Appendix A1). Most Ukaliq ultramafic rocks are distinguished by high Al/Ti and low Gd/Yb ratios and, overall, are compositionally similar to Al-enriched komatiites (Appendix A1) (Arndt et al., 2008). Their high degree of serpentinization and metasomatism expected to occur during hydrothermal alteration renders these rocks poorly suited for ^{147}Sm-^{143}Nd studies. Thus, with the exception of one relatively well preserved pyroxenite, and two hornblendites sampled near the top of the main ultramafic body, this category of rock samples are not further considered in this study.

Mafic lithologies of the USB display a wide compositional range, with SiO_2=46-53 wt%, MgO=7-12 wt% and CaO=4-12 wt% (Fig. 2, Appendix A2). Most samples define a trend of decreasing

incompatible elements (e.g. ΣREE) with increasing SiO_2 content (Fig. 2), which cannot be described as a magmatic differentiation trend and suggests the presence of distinct primary magma compositions. The major and trace element characteristics, in conjunction with petrographic examination of thin sections, contributes to distinguishing four subtypes of mafic rocks within this outcrop, hereafter referred to as *tholeiitic*, *transitional*, *boninitic* and *enriched*. The main characteristics of these four groups are illustrated in plots of Al/Ti versus selected major and trace elements in Fig. 2, and can be summarized as follows;

Tholeiitic lavas (N=9) have low SiO_2 content (46-49 wt%) and Al_2O_3/TiO_2 ratios ranging from 10 to 20. With the exception of one specimen with anomalously high SiO_2, this group is fairly homogeneous, with CaO≈10 wt%, MgO≈8 wt%, Al_2O_3≈15 wt% and Fe_2O_3≈12-15 wt%. Despite low Silica contents, samples show the highest overall abundance of incompatible elements, with ΣREE=25-60 ppm and TiO_2=0.7-1.3 wt%, consistent with derivation of their parent magma from a relatively fertile mantle source. Samples from this group have flat chondrite-normalized REE patterns (Appendix A2), exhibit a slight depletion in LILE and show little or no HFSE anomaly.

Boninitic lavas (N=5), in contrast, have markedly higher SiO_2 content (50-53 wt%) and Al_2O_3/TiO_2 ratios (27-30) associated with low CaO (5 wt%) and high MgO (12 wt%) contents. This group has the lowest overall abundance of incompatible elements (ΣREE=20-30 ppm, TiO_2=0.5 wt%), is markedly enriched in Cr (up to 800 ppm), and exhibits a concave upward trace element pattern with sub-chondritic $(Gd/Yb)_N$ and super-chondritic $(La/Sm)_N$=1.5-1.9. Trace element patterns show pronounced negative Nb-Ta anomalies ($(Nb/Th)_N$≈0.3), and slight excesses of Zr compared to the adjacent REE. The major and trace element characteristics of this group are reminiscent of modern low-Ca boninites (Crawford et al., 1989), although only 2 out of 5 samples have SiO_2 contents high enough to classify as *sensu stricto* boninites according to the IUGS nomenclature (Le Bas, 2000).

Intermediate between tholeiitic and boninitic lavas, *the 'transitional'* group (N=5) is characterized by Al_2O_3/TiO_2 ratio typically ranging between 20 and 25, and SiO_2 content between 48-50 wt%. Samples

from this group exhibit low Nb/Th and high Th/Yb ratios similar to the boninitic lavas, and their major element composition is essentially identical to the tholeiitic group, albeit with lower TiO_2 (and ΣREE) contents suggestive of a more refractory mantle source.

Lastly, a single specimen (IN12032), hereafter referred to as *enriched metabasalt*, is characterized by high SiO_2 (52 wt%), together with high REE content (ΣREE=52 ppm), and a marked enrichment in LILE ($(Th/Yb)_N$=5.9). The sample displays negative Nb and Ti anomalies reminiscent of magmas from modern calc-alkaline series, although its FeO/MgO ratio of 1.6 does not place it unambiguously within the calc-alkaline field of the Miyashiro diagram. As will be discussed later (section 5), the major and trace element chemistry of this sample point either towards assimilation of a tonalitic contaminant at crustal level, or metasomatic enrichment of a depleted mantle source by tonalitic melts.

Overall, the geochemistry of Ukaliq amphibolites closely resembles that described for “metabasalts” in Nuvvuagittuq. Tholeiitic and transitional amphibolites from our outcrops would fall into what has been termed in the NSB as the "High-Ti" group, while the enriched and boninitic lavas are similar to the "enriched low-Ti" and "depleted low-Ti" groups, respectively (O’Neil et al., 2011). Ukaliq lavas, therefore, appear to bear some relation to the cummingtonite-amphibolites at Nuvvuagittuq. They nevertheless display less compositional heterogeneity, most likely reflecting a different alteration history, than their respective equivalents in the NSB. Specifically, the exposed lithologies show no evidence for secondary loss of Ca and Na (Fig. 2C), suggesting that the hydrothermal event proposed to have mobilized all but the most immobile elements in NSB mafic protoliths (Cates et al., 2013) did not affect the Ukaliq rocks. While our USB samples show local evidence for secondary silicification and metasomatism, they define coherent compositional fields, which we conclude are more likely than the highly altered NSB cummingtonite-amphibolites to reflect primary characteristics of their parent magmas.

3.2. Chemical sediments (Quartzites and BIFs)

Magnetite-bearing rocks of chemical sedimentary origin occur both on the Eastern side of the sequence, as a discontinuous Si-rich layer locally grading into cherty units, and on the Western side, as a nearly continuous 50 cm-1 m wide Fe-rich layer of probable BIF protolith interleaved with mafic rocks (Fig. 1). The specimen sampled on the Eastern side has high SiO_2 content (89 wt%) and low Fe_2O_3 (8.5 wt%), with all other oxides below or equal to 1 wt%. BIFs sampled on the Western side have high Fe_2O_3 contents (35-70 wt%), MgO=4-7 wt% and Al_2O_3=0.6-2 wt%. All samples display shale-normalized REE+Y patterns typical of Archean marine sediments, marked by a depletion of LREE compared to HREE, small positive Eu anomalies and elevated Y/Ho ratios (Fig. 3).

4. Results

^{146,147}Sm-^{142,143}Nd results for 21 amphibolites, 2 hornblendites, 1 pyroxenite, 14 granitoid gneisses and 11 chemical sediments of the Ukaliq belt and surrounding Innuksuac complex are summarized in Table 1 and Figure 4. Individual analyses for samples and standards, as well as analytical methods employed for ^{147}Sm-^{143}Nd and ^{142}Nd analyses are provided in Appendix A3-4. Reproducibility of the JNdi standard during the course of this study was on average of ±3 ppm (2.S.D.) (Appendix A3). Variations of the ^{142}Nd/^{144}Nd ratio, noted as μ^{142}Nd, are expressed as relative deviations (in ppm) with regards to the JNdi standard. Variations of the ^{143}Nd/^{144}Nd ratio are expressed using the conventional ε notation, after normalization to the CHUR value (Bouvier et al., 2008). Throughout the paper, ^{146}Sm-^{142}Nd ages are calculated using an initial ^{146}Sm/^{144}Sm ratio of 0.0082 and a half-life of 103 Ma (Meissner et al., 1987; Marks et al., 2014). Alternative ages calculated using a half-life of 68 Ma for ^{146}Sm (Kinoshita et al., 2012) are also provided in parenthesis, in which case the initial ^{146}Sm/^{144}Sm ratio was adjusted to 0.0094. Unless stated otherwise, errors are provided as 2 S.D.

4.1. Amphibolites and ultramafic rocks

As shown in Figure 4, each group of mafic/ultramafic rocks is characterized by a distinct and internally homogeneous ^{142}Nd signature. Tholeiitic and ultramafic lavas have μ^{142}Nd within error of the modern mantle value, at -1.3±2.8 ppm and -0.8±0.4 ppm, respectively. In contrast, the boninitic and transitional lavas exhibit similar negative effects at -4.1±1.6 ppm and -4.7±2.8 ppm. Lastly, the enriched amphibolite (IN12032) exhibits the lowest μ^{142}Nd signature at -9.4±3 ppm. When plotted in a ^{142}Nd/^{144}Nd vs Sm/Nd space (Fig. 5A), mafic rocks define a rough positive correlation which, if considered as an isochron relationship, yields an apparent emplacement age of 4215^{+50}_{-76} Ma, (*or* 4321^{+33}_{-50} *Ma using* $T_{1/2}$*=68 Ma*). This result is similar to that obtained from mafic samples of the NSB (O'Neil et al., 2008; Roth et al., 2013), confirming the close relationship between Ukaliq and Nuvvuagittuq.

The ^{147}Sm-^{143}Nd results obtained from Ukaliq lavas (Fig. 5B) show substantial excess scatter and, overall, provide an imprecise date of 3903±250 Ma. Eliminating samples showing signs of secondary alteration, silicification or K-metasomatism results in a slightly older age estimate at 3963±250 Ma. As for the ^{146}Sm-^{142}Nd array, the slope of the ^{147}Sm-^{143}Nd errorchron is largely controlled by the enriched amphibolite; disregarding this sample yields a younger age of 3735±320 Ma that resembles U-Pb zircon geochronology for the oldest gneissic components of the NSB (Cates and Mojzsis, 2007). Regressions obtained by pooling together samples with identical μ^{142}Nd yield imprecise but similar Eoarchean dates at 3588±410 Ma (tholeiitic and ultramafics) and 3677±480 Ma (transitional and boninitic). Hence, the ^{147}Sm-^{143}Nd systematics do not substantiate a Hadean emplacement age for Ukaliq lavas.

4.2. Plutonic rocks

Tonalitic gneisses sampled in the vicinity of Ukaliq have zircon U-Pb ages ranging from 3.45 Ga to 3.65 Ga, and ^{147}Sm-^{143}Nd model ages (T_{dm}) ranging from 3.3 to 3.9 Ga. With the exception of IN12014,

all TTG gneisses have negative $\varepsilon^{143}Nd_i$ ranging from 0 to -3 ε-units, and all but one sample have negative $\mu^{142}Nd$ averaging -5.6±3.2 ppm. On the other hand, Neoarchean granites have $\mu^{142}Nd$ within error of the modern terrestrial value, despite negative $\varepsilon^{143}Nd_i$ indicative of a crustal precursor. These results confirm the presence of an inherited Hadean component in the Voizel suite, as previously reported by O'Neil et al. (2008) and Roth et al. (2013). This Hadean component, however, does not appear to have been involved in later magmatic events in the area.

4.3. Rocks of chemical sedimentary origin

New $^{146,147}Sm$-$^{142,143}Nd$ analyses for magnetite-bearing rocks of probable BIF protolith from the Nuvvuagittuq, Ukaliq and Isua supracrustal belts are summarized in Figure 4. Nuvvuagittuq BIFs define an imprecise date of 2719±610 Ma, similar to a two-point isochron age, suggesting at least partial isotopic equilibration on a whole-rock scale during metamorphism associated with assembly of NESP terranes in the Neoarchean (Cates and Mojzsis, 2009). Disturbance of the ^{147}Sm-^{143}Nd chronometer in NSB samples with low Nd contents is also evidenced by highly scattered model ages (Fig. 6) which prevents determination of a deposition age using this method. From another standpoint, four USB samples with markedly higher Nd contents yield homogeneous model ages at 3.78-4.07 Ga, similar to the ^{147}Sm-^{143}Nd age derived from mafic/ultramafic samples. Despite variably disturbed ^{147}Sm-^{143}Nd systematics, all samples from Ukaliq and Nuvvuagittuq present identical $\mu^{142}Nd$ within errors of the terrestrial value, at -1.9±2.1 and -2.7±1.3 ppm, respectively. As shown in Figure 5A, BIFs from Ukaliq and Nuvvuagittuq do not plot on the ^{146}Sm-^{142}Nd array defined by volcanic rocks. Their $\mu^{142}Nd$ is constant, irrespective of their Sm/Nd ratio, and identical to that inferred for the Eoarchean ocean from our analyses of Isua BIFs ($\mu^{142}Nd$=-2.4±3 ppm). Thus, despite their stratigraphic relationships with mafic lavas carrying the ^{142}Nd anomalies, chemical sediments in the Ukaliq/Nuvvuagittuq belts show no evidence for in situ decay of ^{146}Sm that would be expected from a Hadean deposition age.

5. Discussion

5.1. Radiogenic vs. inherited ^{142}Nd anomalies

The apparent ^{146}Sm-^{142}Nd and ^{147}Sm-^{143}Nd ages derived from magmatic rocks of the USB, while somewhat less discordant that those obtained for Nuvvuagittuq, remain subject to the same ambiguities raised by previous investigations of the NSB. Since magmas derived from sources with different μ^{142}Nd would also have distinct initial ^{143}Nd/^{144}Nd ratios, all ^{147}Sm-^{143}Nd ages obtained from Ukaliq and Nuvvuagittuq lavas are inherently problematic. Contamination of Eoarchean magmas by a Hadean enriched component would, in fact, generate mixing lines with positive slopes in both the ^{146}Sm-^{142}Nd and ^{147}Sm-^{143}Nd isochron plots. Therefore, even the near-concordant Hadean dates derived from filtered subsets of mafic rocks by O'Neil et al. (2012) are ambiguous, consistent either with a Hadean emplacement age or the presence of an inherited component within younger lavas. The geochronological significance of any Sm-Nd results for these rocks is further obscured by the fact that the major and trace element variability observed in mafic lavas, and therefore most of the observed spread in Sm/Nd, is not primarily controlled by magmatic differentiation but most likely by source heterogeneities (Section 5.3). These observations preclude a straightforward age determination from either the ^{146}Sm-^{142}Nd or ^{147}Sm-^{143}Nd chronometers. Examination of the fine structure of the ^{142,143}Nd signal, however, reveals several key features that consistently point towards an inherited origin for the negative anomalies in Ukaliq lavas. First, ^{147}Sm-^{143}Nd regressions obtained by pooling samples with identical ^{142}Nd/^{144}Nd (and, arguably, identical initial ^{143}Nd/^{144}Nd), yield imprecise but clearly *younger* ages than that obtained from the ^{146}Sm-^{142}Nd array (Section 4.1.). Second, the presence of ^{142}Nd anomalies appears to be mainly restricted to lavas with boninitic affinities, suggesting derivation from a metasomatically enriched mantle source (section 5.3.). In contrast, tholeiitic and ultramafic rocks have constant μ^{142}Nd irrespective of their Sm/Nd ratio (Fig. 5A). Lastly, our results on chemical sediments of the USB and NSB are difficult to reconcile with a

Hadean emplacement age. BIFs have low Sm/Nd ratios that reflect on the predominantly crustal origin of REE in seawater (e.g. Mloszewska et al., 2013), so that deposition before 4.1 Gyr ago is expected to have resulted in the production of significant ^{142}Nd anomalies (typically -10 ppm for a 4.25 Ga deposition age). The BIFs of the USB and NSB, however, show no statistically resolvable effect. Their μ^{142}Nd is indistinguishable from the signature of Eoarchean seawater, as inferred from the Isua BIFs analyses. We conclude that this observation is inconsistent with deposition of BIF protoliths at a time when ^{146}Sm was still extant.

The lack of ^{142}Nd anomalies in chemical sediments of the Ukaliq/Nuvvuagittuq belts has profound implications for the geochronology of supracrustal enclaves in the Innuksuac complex. Chemical sediments in both belts are stratigraphically interleaved with mafic lavas carrying variable ^{142}Nd anomalies (Mloszewska et al., 2012; O'Neil et al., 2011). Further, field observations revealed no evidence for tectonic intercalation of the BIFs within the associated mafic/ultramafic sequences. Hence, the lack of unradiogenic effects despite low Sm/Nd ratios characterizing these lithologies cannot be explained by late sedimentation on a pre-existing Hadean mafic crust. While samples with low Nd content show evidence for late disturbance of the ^{147}Sm-^{143}Nd system, the Ukaliq BIFs with high Nd content yield Eoarchean model ages consistent with U-Pb zircon geochronology, and show no compelling evidence for isotopic resetting during Neoarchean metamorphism. Thus, while it is difficult to entirely disprove the possibility of open system behavior of the ^{146}Sm-^{142}Nd system in BIFs, we believe that the similarity between Isua, Ukaliq and Nuvvuagittuq samples is more than mere coincidence. The most plausible interpretation is that chemical sediments that are found interleaved within the Ukaliq/Nuvvuagittuq sequences deposited at a time when ^{146}Sm was extinct, from an Eoarchean ocean isotopically identical to, or possibly slightly less radiogenic than the modern mantle. Given their stratigraphic relationship with the surrounding mafic lava flows, the lack of unradiogenic effects in BIFs strengthens the case for an inherited origin of the ^{142}Nd anomalies in volcanic rocks of the Innuksuac complex.

5.2. Age of the Hadean enriched reservoir

Due to the short lifetime of ^{146}Sm, the presence of ^{142}Nd heterogeneities in Ukaliq/Nuvvuagittuq lavas constitutes straightforward evidence that Hadean material was involved in the genesis of the oldest components of the Innukjuak domain. More quantitative age constraints cannot be derived from the slope of the ^{146}Sm-^{142}Nd array, as the latter reflects a mixture of Hadean and Eoarchean components and is therefore chronologically meaningless. Nevertheless, a model age of differentiation can be derived for the Hadean enriched precursor, using a combination of the ^{146}Sm-^{142}Nd and ^{147}Sm-^{143}Nd chronometers (e.g. Caro, 2011). Model age calculations using the coupled ^{146,147}Sm-^{142,143}Nd system have the advantage of being solely based on the isotopic composition of the rocks and do not rely on their Sm/Nd ratios. Using a simple set of chronometric equations, ^{146,147}Sm-^{142,143}Nd systematics can provide a model age of differentiation (T_d) and an estimate of the time-integrated ^{147}Sm/^{144}Nd ratio of the reservoir in which the ^{142}Nd anomaly was initially produced.

Following previous ^{146,147}Sm-^{142,143}Nd studies, we make the simplifying assumption that the Hadean reservoir carrying the ^{142}Nd anomaly was generated at time T_d from an initially primitive mantle, and subsequently evolved as closed system until it was sampled in the Eoarchean, when ^{146}Sm was no longer extant. We consider an eruption age of 3.75 Ga for Ukaliq lavas, as inferred from previous U-Pb zircon studies in the NSB (Augland and David, 2015; Cates and Mojzsis, 2007; Cates et al., 2013; David et al., 2006), and use the composition of IN12032 (μ^{142}Nd=-9.8 ppm and $\varepsilon^{143}Nd_i$=-2) as the closest approximation of the Hadean component. With these input parameters, the model age of differentiation for the Ukaliq enriched source is estimated to be $4.36^{+0.05}_{-0.06}$ Ga (or $4.44^{+0.03}_{-0.04}$ Ga using a 68 Ma half-life for ^{146}Sm). By comparison, the Isua mantle source is estimated to have differentiated $4.42^{+0.05}_{-0.06}$ Ga ago (Caro et al., 2006; Rizo et al 2011), which is only marginally older than the estimated age of crystallization of the lunar magma ocean, at $4.39^{+0.016}_{-0.014}$ Ga (Mcleod et al., 2014). As shown in Figure 7, a regression including the ^{142,143}Nd data for Ukaliq and Isua supracrustal belts yields an age

of $4.39^{+0.04}_{-0.035}$ Ga, which is similar to the model age derived from IN12032 and virtually identical to the estimated age of differentiation of the lunar mantle.

It is important to recognize that the chronological information derived from ^{146,147}Sm-^{142,143}Nd systematics is a model age and, as such, depends on the compositional model assumed for the Bulk Silicate Earth (BSE). The ages provided above were calculated assuming that the BSE has a chondritic Sm/Nd ratio (^{147}Sm/^{144}Nd=0.1960, Bouvier et al., 2008) and a ^{142}Nd/^{144}Nd ratio identical to that of the modern mantle (i.e. $\mu^{142}Nd_{BSE}$=0). However, alternative models involving slightly superchondritic Sm/Nd compositions have been proposed based on the meteoritic ^{142}Nd record (e.g. Boyet and Gannoun, 2013; Caro et al., 2008; Jackson and Jellinek, 2013; O'Neill and Palme, 2008; Qin et al., 2011; Caro, 2015). As shown in Figure 7B, a superchondritic Sm/Nd ratio for the BSE would tend to generate older model ages for the Isua depleted source, and younger ages for the Ukaliq enriched source. Therefore, the apparent synchronous differentiation of Ukaliq and Isua parent reservoirs remains, to a certain extent, model dependent. Solving this issue requires precise assessment of the role of nucleosynthetic vs. radiogenic processes in generating the chondritic ^{142}Nd signal, which is analytically challenging due to the small magnitude of the measured anomalies. However, recent studies suggest that the offset between the terrestrial and chondritic ^{142}Nd/^{144}Nd ratios may be entirely accounted for by nucleosynthetic processes (Fukai and Yokoyama, 2016; Burckhardt et al., 2016), in which case the chronological results shown in Figure 7 would apply. A single, large-scale differentiation event ca. 4.4 Gyr ago would then best account for the ^{142,143}Nd signatures recorded in both the Ukalik/Nuvvuagittuq and Isua rocks.

The presence of positive ^{142}Nd anomalies in the Eoarchean mantle is generally viewed as reflecting magma ocean crystallization in the aftermath of the Moon-forming giant impact (e.g. Caro, 2011; Caro et al., 2005; Debaille et al., 2013; Bennett et al., 2007; Boyet et al., 2003). This interpretation relies on the estimated age of differentiation, which fits independently derived constraints on the timescale of terrestrial accretion, as well as the apparent decoupling of the Lu-Hf and Sm-Nd systems

in the Isua mantle source; an expected outcome of Mg-perovskite crystallization in a deep magma ocean (Caro et al., 2005; Rizo et al., 2011). A synchronous differentiation of the Ukaliq and Isua sources would thus imply contamination of former's lavas by material derived from Earth's primordial crust, more than 600 Myr after solidification of the magma ocean. The emplacement of such long-lived, compositionally buoyant lithosphere has been theorized based on parameterized and numerical convection models (Korenaga, 2006; O'Neill et al., 2013; van Hunen and van den Berg, 2008). Due to the sparsity of Hadean components in the geological record, however, its prior existence has proved difficult to substantiate. The chronological constraints derived from ^{146,147}Sm-^{142,143}Nd systematics suggest that Hadean plates stabilized early, and could be preserved from recycling for a period of time much longer than modern oceanic plates. From a geodynamic viewpoint, this would be consistent with a regime of either stagnant-lid (O'Neill and Debaille, 2014) or sluggish plate tectonics (Foley et al., 2014; Korenaga, 2006), but is seemingly at odds with the occurrence of global resurfacing events, or any mechanism involving rapid rejuvenation of the Hadean surface. Overall, our results suggest that hotter mantle temperatures in the Hadean induced a relatively quiescent tectonic regime, characterized by inefficient lithospheric recycling and a long crustal residence time. This quiescent regime, in turn, allowed remnants of Earth's primordial crust to contribute to the genesis of continental terranes in the Eoarchean.

5.3. Composition of the Hadean enriched reservoir

We now turn from the chronological to the petrogenetic implications of our results, focusing on the nature of the Hadean protolith. Of potential importance to this issue is the observation that μ^{142}Nd in Ukaliq lavas show a high degree of covariation with Th/La (Fig. 8A), a trace element ratio usually exhibiting limited variability in mafic lithologies, with the notable exception of arc magmas (Plank, 2005). As Th and La are both highly incompatible, they exhibit similar behavior during partial melting and only experience fractionation during crustal differentiation processes. As a result, the upper

crust is characterized by high Th/La (0.25-0.4), whereas MORBs and most OIBs have Th/La<0.1 (Condie, 1993; Plank, 2005; Taylor and McLennan, 1985). Examination of the Th/La-Sm/La relationships of Figure 8B shows that tholeiitic lavas have low Th/La irrespective of their Sm/La, as observed in modern MORBs. In contrast, lavas exhibiting ^{142}Nd anomalies show a trend of increasing Th/La with decreasing Sm/La, likely reflecting a mixing relationship between the prevalent Eoarchean mantle (or its melting products) and an enriched end-member similar to the average Archean crust. Thus, Ukaliq lavas must have inherited their ^{142}Nd signature from a felsic contaminant, which would be consistent with the reworking of Hadean crustal material in the Innuksuac complex.

By 3.75 Gyr ago, a 4.36 Ga old felsic crust with ^{147}Sm/^{144}Nd=0.08-0.12 would have developed a negative μ^{142}Nd of -20 to -30 ppm (Fig. 7A, model A). As shown in Figures 8A-9, assimilation of such unradiogenic material could readily explain the compositional range of Ukaliq amphibolites. Based on these relationships, the trace element composition of IN12032 can be consistently reproduced by ca. 20 wt% assimilation of a TTG contaminant with μ^{142}Nd = -20 to -30 ppm (Fig. 9B-C). Hence, much of the compositional variability observed in Ukaliq lavas could be accounted for by crustal contamination. It is also well established that such mechanism can generate apparent ^{147}Sm-^{143}Nd dates (and, therefore, ^{146}Sm-^{142}Nd dates) well in excess of true emplacement ages, as illustrated by several case studies of Archean mafic and ultramafic suites (Chauvel et al., 1985; Juteau et al., 1988).

The crustal assimilation model, however, faces several difficulties. First, despite the seemingly simple relationships of Figure 9, neither the boninitic nor the transitional lavas can be generated by crustal contamination starting from the most primitive tholeiitic composition. This is most evident for boninitic lavas, which exhibits Mg contents higher than tholeiitic lavas, as well as lower abundances of incompatible elements despite higher SiO_2 contents. Second, the crustal assimilation model requires a contaminant with highly negative μ^{142}Nd. Felsic plutonic rocks currently exposed in the vicinity of the Ukaliq belt, however, average -5.6±3.2 ppm and do not represent plausible contaminants, as is evident in a plot of Th/Yb vs. μ^{142}Nd (Fig. 9B). Lastly, the negative ^{142}Nd effects

observed in Voizel TTGs would imply that their parent magmas assimilated pre-existing Hadean felsic crust in proportions ranging from 15 to 25 wt%. The reworking of older continental crust into younger generations of granitoids is not uncommon, but in the present case appears difficult to reconcile with the striking absence of inherited Hadean zircons in these heavily contaminated rocks (David et al., 2006; Cates and Mojzsis, 2007).

An alternative scenario, more consistent with the above observations, is that Ukaliq lavas inherited their signature from an Eoarchean felsic component derived from a pre-existing Hadean mafic crust. In this case, the ^{142,143}Nd signature of Ukaliq lavas would reflect that of the Hadean precursor, but their high Th/La values would represent a compositional characteristic of the felsic derivatives carrying the negative ^{142}Nd effects. A mafic precursor would be generally consistent with the compositional constraints derived from coupled Sm-Nd systematics (Fig. 7A); using the ^{142,143}Nd signature of the most contaminated sample, the maximum $(^{147}Sm/^{144}Nd)_{srce}$ ratio of the Hadean source is estimated to be 0.17, which falls within the compositional range of mafic/ultramafic rocks (0.15-0.20) (Condie, 1993). As shown in Figure 8D, a 4.36 Ga old mafic crust with $^{147}Sm/^{144}Nd$=0.15-0.17 would have developed by 3.75 Ga a μ^{142}Nd of -10 to -15 ppm (model B), and its felsic derivatives would plot on the μ^{142}Nd-Th/La array defined by Ukaliq lavas (model C, Fig 8C). This scenario would thus satisfy trace element constraints, which require a predominantly felsic contaminant, while circumventing the issues associated with the crustal assimilation model.

The scenarios mentioned above are expected to generate identical effects with regards to trace elements. However, they differ in that a Hadean mafic precursor (and its felsic derivatives (model C)) would have less negative μ^{142}Nd than a felsic crust of the same age (model A). Consequently, a crustal contamination scenario using model C as enriched end-member would require larger amount (>40 wt%) of assimilation to account for the signature of IN12032. The μ^{142}Nd-Th/La systematics of Ukaliq rocks, alternatively, could result from metasomatic enrichment of a depleted or primitive mantle reservoir, prior to extraction of their parent magmas. The isotopic signature of Ukaliq lavas

would then require adding 2-10 wt% of a tonalitic contaminant with μ^{142}Nd=-15 ppm to a mantle with initially primitive abundances of REE.

A key observation in support of a metasomatically enriched mantle source is the widespread occurrence of lavas with boninitic affinities in the Nuvvuagittuq/Ukaliq belts. Boninites are subduction-related volcanic rocks characterized by high SiO_2 (>52 wt%), high MgO (>8 wt%) and low TiO_2 (<0.5 wt%) contents (Crawford et al., 1989; Hickey and Frey, 1982). Their characteristic U-shaped REE patterns and overall low abundances of incompatible elements are taken to reflect addition of subduction fluids/melts to a highly refractory mantle, the formation of which is generally attributed to prior extraction of tholeiitic melts during asthenospheric uplift associated with trench retreat or back-arc spreading (König et al., 2010; Bedard, 1999; Hickey and Frey, 1982). The presence of lavas sharing the geochemical characteristics of modern boninite/tholeiite associations in the NSB has been emphasized in several previous studies (O'Neil et al., 2011; Turner et al., 2014), but the implication of this result for Sm-Nd systematics has received surprisingly little attention. Of central importance is the long recognized observation that most boninite suites define positive correlations in a ^{143}Nd/^{144}Nd vs. Sm/Nd plot (Cameron et al., 1983; Hickey and Frey, 1982; König et al., 2010). These covariations arise from the fact that slab-derived components often contribute >50% of the LREE budget of modern boninites (Cameron et al., 1983; König et al., 2010). A consequence, illustrated in Figure 10C, is that while tholeiitic magmas in fore arcs or subduction-related ophiolites have ε^{143}Nd similar to their coeval mantle, boninites, when present, have variable but always less radiogenic ε^{143}Nd largely inherited from the subducting plate.

It is unclear whether the geochemical features illustrated in Figure 10 must imply the existence of modern-type subduction processes in the Eoarchean, or could have been generated in drip-like downwellings. Nevertheless, in the absence of plausible contaminants in the Innuksuac complex, the isotopic and geochemical characteristics of Ukaliq lavas point towards metasomatic enrichment of a variably depleted Eoarchean mantle as the most plausible scenario for explaining the Innuksuac

^{146}Sm-^{142}Nd array. This inherited signature, in turn, establishes a clear genetic relationship between the foundering of Earth's primordial crust and the emplacement of both plutonic and volcanic rocks in the Innuksuac complex.

6. Conclusions

An intense debate has surrounded the ^{146}Sm-^{142}Nd signature characterizing volcanic rocks of the Nuvvuagittuq supracrustal belt, following O'Neil et al.'s proposal to assign a Hadean emplacement age to the sequence. The highly altered nature of the mafic lithologies carrying the ^{142}Nd anomalies, however, has been an obstacle to geochronological investigations in the NSB, and has led to diverging interpretations of their isotopic record. In this study, we investigated the ^{146,147}Sm-^{142,143}Nd systematics of volcanic and sedimentary rocks from the Ukaliq supracrustal belt, a newly discovered volcano-sedimentary enclave of the Innuksuac complex. Mafic lavas of the USB lack evidence of the hydrothermal alteration that massively modified the chemistry of Nuvvuagittuq rocks and, overall, are in a better state of preservation. They nevertheless display a similar geochemical "flavor", characterized by the association of arc-type volcanic rocks with variably negative ^{142}Nd anomalies. Despite a rough correlation between the ^{142}Nd/^{144}Nd and Sm/Nd ratios, the fine structure of the ^{146}Sm-^{142}Nd signal in Ukaliq rocks is inconsistent with a Hadean emplacement age. ^{142}Nd anomalies are primarily carried by boninitic lavas, likely signaling metasomatic enrichment at mantle depth, whereas the associated tholeiitic and ultramafic rocks have normal ^{142}Nd/^{144}Nd regardless of their Sm/Nd ratio. More importantly, chemical sediments interleaved in the Nuvvuagittuq and Ukaliq sequences lack the negative anomalies that, given their low Sm/Nd ratio, would be expected had these sediments deposited in the Hadean.

Coupled ^{146,147}Sm-^{142,143}Nd chronometry indicates that the Ukaliq/Nuvvuagittuq Hadean source was extracted from the mantle ca. 4.4 Gyr ago, possibly as a result of magma ocean crystallization, and had a predominantly mafic composition. We propose that foundering of this primordial crust after a

long period of quiescence at the surface produced felsic melts and/or fluids carrying unradiogenic ^{142,143}Nd which imprinted the overlying mantle with a chemically and isotopically enriched signature. Metasomatically triggered melting of this modified mantle then generated a variety of boninitic and tholeiitic magmas, the combination of which resulted in the ^{146}Sm-^{142}Nd pseudo-isochrons observed in Ukaliq and Nuvvuagittuq lavas. Beyond their chronological implications, our results provide clear observational evidence for the emplacement of a long-lived lithosphere following solidification of the terrestrial magma ocean. This observation suggests that hotter internal temperatures did not impede the stabilization of Hadean plates. Rather, they reduced the efficiency of lithospheric recycling and favored a more sluggish tectonic style in the post-magma ocean Earth.

Acknowledgments: We thank Dr. Igor Puchtel and an anonymous reviewer for their constructive comments of this paper. Logistical assistance from the Pituvik Landholding Corporation of Nunavik is gratefully acknowledged. A. Schumacher and C. Zimmermann provided assistance with TIMS and ICP-MS work. GC acknowledges financial support from Agence Nationale de la Recherche (Grant ANR-11-JS56-0012 "DESIR"). P.M. was supported by a doctoral fellowship awarded by Région Lorraine. SJM was supported in this work by the NASA Exobiology Program (14-EXO14_2-0050), and from the Collaborative for Research in Origins (CRiO) at the University of Colorado Boulder, which is funded by the John Templeton Foundation-FfAME Origins program (grant id# 15-09-0168).

Figure Captions

Figure 1: (A) Geographical location and geological map of the southern part of the Ukaliq Supracrustal belt showing the main lithological units and sampling sites. GPS coordinates for samples analyzed in this study are provided in the electronic supplement. **(B)** Lithological sections and magnetic susceptibility profiles across the Ukalik belt.

Figure 2: Al_2O_3/TiO_2 vs selected major and trace element in mafic lavas of the Ukaliq and Nuvvuagittuq Supracrustal Belts. Data for the Ukaliq belt are available in electronic supplement. Nuvvuagittuq data are compiled from the literature (Cates and Mojzsis, 2007; Cates et al., 2013; O'Neil et al., 2011, 2008, 2007).

Figure 3: Shale-normalized REE+Y patterns for Ukaliq and Nuvvuagittuq BIFs analyzed in this study. PAAS: Post-Archean Australian Shale.

Figure 4: Summary of ^{142}Nd results for volcanic rocks, plutonic rocks and chemical sediments analyzed in this study. Errors for individual analyses (or individual samples) are given as 2 S.E. Grey fields represent 2 S.D. errors on averages obtained for each lithologic type or location.

Figure 5: (A) ^{146}Sm-^{142}Nd results for volcanic and sedimentary rocks of the Ukaliq and Nuvvuagittuq belts, plotted in a conventional isochron diagram. The grey field represents the 2.S.D error envelope

for the regression on mafic lavas (Sample IN14002 is excluded from regression). **(B)** ^{147}Sm-^{143}Nd errorchron obtained on volcanic rocks of the Ukaliq belt. Both regressions are calculated using Isoplot (Ludwig, 1991).

Figure 6: Depleted Mantle model ages (T_{DM}) for BIFs of the Ukaliq and Nuvvuagittuq belts. Note that most samples show a trend of decreasing model ages with decreasing Nd content, consistent with open system behavior during late metamorphic events. Samples with high Nd abundances from the Ukaliq belt define a narrower age range, consistent with closed-system behavior since 3.8-4 Ga.

Figure 7: (A) Coupled $^{146,147}Sm$-$^{142,143}Nd$ systematics for magmatic rocks of the Ukaliq belt and surrounding TTGs of the Voizel suite. The $^{142,143}Nd$ systematics of Isua supracrustal belt (3.7-3.8 Ga; Caro et al. (2006)) are shown for comparison. The dashed curves represent loci of constant $(^{147}Sm/^{144}Nd)_{source}$ ratios, ranging from 0.13 to 0.24, in the Hadean source. Solid lines are loci of constant model ages, ranging from 4.1 Ga to 4.567 Ga. The thick black line represents a linear regression including Isua and Ukaliq data. **(B)** Dependence of the calculated model ages for Isua and Ukaliq sources on the BSE Sm/Nd ratio. All ages are calculated using a half-life of 103 Ma for ^{146}Sm. Ages calculated using a half-life of 68 Ma are provided in the text.

Figure 8: (A) $\mu^{142}Nd$ vs. Th/La in amphibolites of the Ukaliq belt. The grey field represents the 2 S.D. error envelope for the linear regression obtained from mafic lavas (one datapoint excluded from regression). The pink curve represents a mixing relationship between the most primitive tholeiitic composition and a crustal end-member with $\mu^{142}Nd$ =-30 ppm and a Th/La ratio of 0.26, corresponding to the average Archean crust (Condie, 1993; Taylor and McLennan, 1985). Numbers in italic represent the mass fraction of assimilated felsic crust. **(B)** Th/La versus Sm/La in Ukaliq mafic

lavas. The compositional fields for modern MORBS and OIBs (Plank, 2005), as well as the Archean and modern upper continental crust (Condie, 1993; Taylor and McLennan, 1985) are shown for comparison. A linear regression through boninitic and enriched lavas intersects the average composition of the Archean crust, suggesting that the carrier of the negative ^{142}Nd anomalies was a LREE-enriched felsic component. **(C)** Location of the possible enriched end-members in a μ^{142}Nd-ε^{143}Nd plot. Model A shows the expected composition of 4.36 Ga old felsic crust with ^{147}Sm/^{144}Nd=0.08-0.12 (Condie, 1993; Taylor and McLennan, 1985). Model B represents the composition of a 4.36 Ga mafic crust with ^{147}Sm/^{144}Nd=0.15-0.17. **(D)** Location of proposed Hadean end-members in a μ^{142}Nd vs Th/La diagram. Model C shows the expected composition of felsic products derived from a 4.36 Ga mafic crust, after extinction of ^{146}Sm.

Figure 9: (A) Th/Yb vs Nb/Th, **(B)** μ^{142}Nd vs Th/Yb and **(C)** μ^{142}Nd vs SiO_2 in mafic lithologies of the Ukaliq belt. The solid pink curves represent mixing relationships between the most primitive tholeiitic composition and a crustal component defined by the average our analyses of Voizel TTGs. The grey fields in panel (B) and (C) represent the compositional range for tholeiitic magmas contaminated by a 4.36 Ga tonalitic crust with μ^{142}Nd ranging from -20 ppm (upper dashed curve) to -30 ppm (lower dashed curve). Numbers in italic represent the mass fraction of assimilated felsic material.

Figure 10: Trace element and isotopic systematics of boninites and tholeiitic basalts in the Marianna fore-arc **(A-C)**, compared to those of the boninitic and tholeiitic groups in the Ukaliq belt **(C-D)**. Data for the Marianna fore arc lavas are from Reagan et al. (2010)**.** Similar relationships were also reported from several boninite suites worldwide (Cameron et al., 1983; Hickey and Frey, 1982; König et al., 2010)**.**

Appendix A: Supplementary material

A1: GPS coordinates and major and trace element data for samples analyzed in this study (Tables SM1-4).

A2: Major and trace element plots for mafic lithologies of the Ukalik belt (Figures SM1-2).

A3: Analytical methods for ^{147}Sm-^{143}Nd and ^{142}Nd analyses

A4: ^{142}Nd analyses for samples and standards (Tables SM6-7)

References

Arndt, N., Lesher, M., Barnes, S.J., 2008. Komatiite. Cambridge University Press, Cambridge, U.K.

Augland, L.E., David, J., 2015. Protocrustal evolution of the Nuvvuagittuq Supracrustal Belt as determined by high precision zircon Lu–Hf and U–Pb isotope data. Earth Planet. Sci. Lett. 428, 162–171. doi:10.1016/j.epsl.2015.07.039

Bedard, J.H., 1999. Petrogenesis of Boninites from the Betts Cove Ophiolite, Newfoundland, Canada : Identification of Subducted Source Components. J. Petrol. 40, 1853–1889.

Bédard, J.H., Brouillette, P., Madore, L., Berclaz, A., 2003. Archaean cratonization and deformation in the northern Superior Province, Canada: an evaluation of plate tectonic versus vertical tectonic models. Precambrian Res. 127, 61–87. doi:10.1016/S0301-9268(03)00181-5

Bennett, V.C., Brandon, A.D., Nutman, A.P., 2007. Coupled ^{142}Nd-^{143}Nd isotopic evidence for Hadean mantle dynamics. Science. 318, 1907–1910.

Bourdon, B., Caro, G., 2007. The early terrestrial crust. Comptes Rendus - Geosci. 339, 928–936. doi:10.1016/j.crte.2007.09.002

Bouvier, A., Vervoort, J.D., Patchett, P.J., 2008. The Lu-Hf and Sm-Nd isotopic composition of CHUR: Constraints from unequilibrated chondrites and implications for the bulk composition of terrestrial planets. Earth Planet. Sci. Lett. 273, 48–57. doi:10.1016/j.epsl.2008.06.010

Boyet, M., Carlson, R.W., 2005. ^{142}Nd Evidence for Early (>4.53 Ga) Global Differentiation of the Silicate Earth. Science. 309, 576–581. doi:10.1126/science.1113634

Boyet, M., Blichert-Toft, J., Rosing, M., Storey, M., Télouk, P., Albarède, F., 2003. ^{142}Nd evidence for early Earth differentiation. Earth Planet. Sci. Lett. 214, 427–442. doi:10.1016/S0012-821X(03)00423-0

Boyet, M., Gannoun, A., 2013. Nucleosynthetic Nd isotope anomalies in primitive enstatite chondrites. Geochim. Cosmochim. Acta 121, 652–666. doi:10.1016/j.gca.2013.07.036

Burkhardt, C., Borg, L.E., Brennecka, Q.R., Shollenberger, Q.R., Dauphas, N., Kleine, T., 2016. Meteoritic Nd isotope constraints on the origin and composition of the Earth. Lunar and Planetary Science Abstracts, 47, p. 190.

Cameron, W.E., McCulloch, M.T., Walker, D.A., 1983. Boninite petrogenesis: Chemical and Nd-Sr isotopic constraints. Earth Planet. Sci. Lett. 65, 75–89. doi:10.1016/0012-821X(83)90191-7

Caro, G., 2015. Chemical geodynamics in a non-chondritic Earth, in: Khan, A., Deschamps, F. (Eds.), The Earth's Heterogeneous Mantle. Springer Geophysics, pp. 329–366.

Caro, G., 2011. Early Silicate Earth Differentiation. Annu. Rev. Earth Planet. Sci. 39, 31–58. doi:10.1146/annurev-earth-040610-133400

Caro, G., Bourdon, B., Birck, J.L., Moorbath, S., 2006. High-precision $^{142}Nd/^{144}Nd$ measurements in terrestrial rocks: Constraints on the early differentiation of the Earth's mantle. Geochim. Cosmochim. Acta 70, 164–191. doi:10.1016/j.gca.2005.08.015

Caro, G., Bourdon, B., Birck, J.-L., Moorbath, S., 2003. ^{146}Sm-^{142}Nd evidence from Isua metamorphosed sediments for early differentiation of the Earth's mantle. Nature 423, 428–432. doi:10.1038/nature01897

Caro, G., Bourdon, B., Halliday, A.N., Quitté, G., 2008. Super-chondritic Sm/Nd ratios in Mars, the Earth and the Moon. Nature 452, 336–339. doi:10.1038/nature06760

Caro, G., Bourdon, B., Wood, B.J., Corgne, A., 2005. Trace-element fractionation in Hadean mantle generated by melt segregation from a magma ocean. Nature 436, 246–249. doi:10.1038/nature03827

Cates, N.L., Mojzsis, S.J., 2009. Metamorphic zircon, trace elements and Neoarchean metamorphism in the ca. 3.75 Ga Nuvvuagittuq supracrustal belt, Québec (Canada). Chem. Geol. 261, 99–114. doi:10.1016/j.chemgeo.2009.01.023

Cates, N.L., Mojzsis, S.J., 2007. Pre-3750 Ma supracrustal rocks from the Nuvvuagittuq supracrustal belt, northern Québec. Earth Planet. Sci. Lett. 255, 9–21. doi:10.1016/j.epsl.2006.11.034

Cates, N.L., Ziegler, K., Schmitt, A.K., Mojzsis, S.J., 2013. Reduced, reused and recycled: Detrital zircons define a maximum age for the Eoarchean (ca. 3750–3780Ma) Nuvvuagittuq Supracrustal Belt, Québec (Canada). Earth Planet. Sci. Lett. 362, 283–293. doi:10.1016/j.epsl.2012.11.054

Chauvel, C., Dupré, B., Jenner, G.A., 1985. The Sm-Nd age of Kambalda volcanics is 500 Ma too old! Earth Planet. Sci. Lett. 74, 315–324. doi:10.1016/S0012-821X(85)80003-0

Condie, K.C., 1993. Chemical composition and evolution of the upper continental crust: Contrasting results from surface samples and shales. Chem. Geol. 104, 1–37. doi:10.1016/0009-2541(93)90140-E

Crawford, A.J., Fallon, T.J., Green, D.H., 1989. Classification, petrogenesis and tectonic setting of boninites, in: Crawford, A.J. (Ed.), Boninites. pp. 1–49.

Darling, J.R., Moser, D.E., Heaman, L.M., Davis, W.J., O'Neil, J., Carlson, R., 2013. Eoarchean to Neoarchean evolution of the Nuvvuagittuq Supracrustal belt: New insights from U-Pb zircon geochronology. Am. J. Sci. 313, 844–876. doi:10.2475/09.2013.02

David, J., Godin, L., Stevenson, R.K., O'Neil, J., Francis, D., 2006. U-Pb ages (3.8–2.7 Ga) and Nd isotope data from the newly identified Eoarchean Nuvvuagittuq supracrustal belt, Superior Craton, Canada. Geol. Soc. Am. Bull. 121, 150–163. doi:10.1130/B26369.1

Debaille, V., O'Neill, C., Brandon, A.D., Haenecour, P., Yin, Q.-Z., Mattielli, N., Treiman, A.H., 2013. Stagnant-lid tectonics in early Earth revealed by ^{142}Nd variations in late Archean rocks. Earth Planet. Sci. Lett. 373, 83–92. doi:10.1016/j.epsl.2013.04.016

Foley, B.J., Bercovici, D., Elkins-Tanton, L.T., 2014. Initiation of plate tectonics from post-magma ocean thermochemical convection. J. Geophys. Res. Solid Earth 119, 8538:8561.

Fukai, R., Yokoyama, T. 2016. Nucleosynthetic Neodymium isotope anomalies in carbonaceous and ordinary chondrites. Lunar and Planetary Science Abstracts, 47, p. 1298.

Guitreau, M., Blichert-Toft, J., Mojzsis, S.J., Roth, A.S.G., Bourdon, B., 2013. A legacy of Hadean silicate differentiation inferred from Hf isotopes in Eoarchean rocks of the Nuvvuagittuq supracrustal belt (Québec, Canada). Earth Planet. Sci. Lett. 362, 171–181. doi:10.1016/j.epsl.2012.11.055

Guitreau, M., Blichert-Toft, J., Mojzsis, S.J., Roth, A.S.G., Bourdon, B., Cates, N.L., Bleeker, W., 2014. Lu–Hf isotope systematics of the Hadean–Eoarchean Acasta Gneiss Complex (Northwest Territories, Canada). Geochim. Cosmochim. Acta 135, 251–269. doi:10.1016/j.gca.2014.03.039

Harper, C.L., Jacobsen, S.B., 1992. Evidence from coupled ^{147}Sm-^{143}Nd and ^{146}Sm-^{142}Nd systematics for very early (4.5-Gyr) differentiation of the Earth's mantle. Nature 360, 728-732. doi:10.1038/360728a0

Harrison, T.M., 2009. The Hadean Crust: Evidence from >4 Ga Zircons. Annu. Rev. Earth Planet. Sci. 37, 479–505. doi:10.1146/annurev.earth.031208.100151

Hickey, R.L., Frey, F.A., 1982. Geochemical characteristics of boninite series volcanics: implications for their source. Geochim. Cosmochim. Acta 46, 2099–2115. doi:10.1016/0016-7037(82)90188-0

Jackson, M.G., Jellinek, A.M., 2013. Major and trace element composition of the high ^{3}He/^{4}He mantle: Implications for the composition of a nonchonditic Earth. Geochemistry, Geophys. Geosystems 14, 2954–2976. doi:10.1002/ggge.20188

Johnson, T.E., Brown, M., Kaus, B.J.P., VanTongeren, J.A., 2013. Delamination and recycling of Archaean crust caused by gravitational instabilities. Nat. Geosci. 7, 47–52. doi:10.1038/ngeo2019

Juteau, M., Pagel, M., Michard, A., Albarede, F., 1988. Assimilation of continental crust by komatiites in the Precambrian basement of the Carswell structure (Saskatchewan, Canada). Contrib. to Mineral. Petrol. 99, 219–225. doi:10.1007/BF00371462

Kinoshita, N., Paul, M., Kashiv, Y., Collon, P., Deibel, C.M., DiGiovine, B., Greene, J.P., Henderson, D.J., Jiang, C.L., Marley, S.T., Nakanishi, T., Pardo, R.C., Rehm, K.E., Robertson, D., Scott, R., Schmitt, C., Tang, X.D., Vondrasek, R., Yokoyama, A., 2012. A Shorter ^{146}Sm Half-Life Measured and Implications for ^{146}Sm-^{142}Nd Chronology in the Solar System. Science. 335, 1614–1617. doi:10.1126/science.1215510

König, S., Münker, C., Schuth, S., Luguet, A., Hoffmann, J.E., Kuduon, J., 2010. Boninites as windows into trace element mobility in subduction zones. Geochim. Cosmochim. Acta 74, 684–704. doi:10.1016/j.gca.2009.10.011

Korenaga, J., 2006. Archean geodynamics and the thermal evolution of Earth. Archean Geodyn. Environ. 164, 7–32. doi:10.1029/164gm03

Le Bas, M.J., 2000. IUGS Reclassification of the High-Mg and Picritic Volcanic Rocks. J. Petrol. 41, 1467–1470. doi:10.1093/petrology/41.10.1467

Ludwig, K.R., 1991. ISOPLOT; a plotting and regression program for radiogenic-isotope data; version 2.53. Open-File Rep.

Marks, N.E., Borg, L.E., Hutcheon, I.D., Jacobsen, B., Clayton, R.N., 2014. Samarium – neodymium chronology and rubidium – strontium systematics of an Allende calcium – aluminum-rich inclusion with implications for ^{146}Sm half-life. Earth Planet. Sci. Lett. 405, 15–24. doi:10.1016/j.epsl.2014.08.017

Mcleod, C.L., Brandon, A.D., Armytage, R.M.G., 2014. Constraints on the formation age and evolution of the Moon from ^{142}Nd–^{143}Nd systematics of Apollo 12 basalts. Earth Planet. Sci. Lett. 396, 179–189. doi:10.1016/j.epsl.2014.04.007

Meissner, F., Schmidt-Ott, W.-D., Ziegeler, L., 1987. Half-life and α-ray energy of ^{146}Sm. Zeitschrift fur Phys. A At. Nucl. 327, 171–174. doi:10.1007/BF01292406

Mloszewska, A.M., Mojzsis, S.J., Pecoits, E., Papineau, D., Dauphas, N., Konhauser, K.O., 2013. Chemical sedimentary protoliths in the >3.75 Ga Nuvvuagittuq Supracrustal Belt (Québec, Canada). Gondwana Res. 23, 574–594. doi:10.1016/j.gr.2012.11.005

Mloszewska, A.M., Pecoits, E., Cates, N.L., Mojzsis, S.J., O'Neil, J., Robbins, L.J., Konhauser, K.O., 2012. The composition of Earth's oldest iron formations: The Nuvvuagittuq Supracrustal Belt (Québec, Canada). Earth Planet. Sci. Lett. 317-318, 331–342. doi:10.1016/j.epsl.2011.11.020

Mojzsis, S.J., Harrison, T.M., Pidgeon, R.T., 2001. Oxygen-isotope evidence from ancient zircons for liquid water at the Earth's surface 4,300 Myr ago. Nature 409, 178–181. doi:10.1038/35051557

O'Neil, J., Carlson, R.W., Francis, D., Stevenson, R.K., 2008. Neodymium-142 Evidence for Hadean Mafic Crust. Science. 321, 1828–1831.

O'Neil, J., Carlson, R.W., Paquette, J.-L., Francis, D., 2012. Formation age and metamorphic history of the Nuvvuagittuq Greenstone Belt. Precambrian Res. 220-221, 23–44. doi:10.1016/j.precamres.2012.07.009

O'Neil, J., Francis, D., Carlson, R.W., 2011. Implications of the Nuvvuagittuq Greenstone Belt for the Formation of Earth's Early Crust. J. Petrol. 52, 985–1009. doi:10.1093/petrology/egr014

O'Neil, J., Maurice, C., Stevenson, R.K., Larocque, J., Cloquet, C., David, J., Francis, D., 2007. The Geology of the 3.8 Ga Nuvvuagittuq (Porpoise Cove) Greenstone Belt, Northeastern Superior Province, Canada, in: Van Kranendonk, M.J., Smithies, R.H., Bennett, V.S. (Eds.), Earth's Oldest Rocks. Elsevier, pp. 219–250. doi:10.1016/S0166-2635(07)15034-9

O'Neil, J., Boyet, M., Carlson, R.W., Paquette, J.-L., 2013. Half a billion years of reworking of Hadean mafic crust to produce the Nuvvuagittuq Eoarchean felsic crust. Earth Planet. Sci. Lett. 379, 13–25. doi:10.1016/j.epsl.2013.07.030

O'Neill, C., Debaille, V., 2014. The evolution of Hadean–Eoarchaean geodynamics. Earth Planet. Sci. Lett. 406, 49–58. doi:10.1016/j.epsl.2014.08.034

O'Neill, C., Debaille, V., Griffin, W., 2013. Deep earth recycling in the Hadean and constraints on surface tectonics. Am. J. Sci. 313, 912–932. doi:10.2475/09.2013.04

O'Neill, H.S.C., Palme, H., 2008. Collisional erosion and the non-chondritic composition of the terrestrial planets. Philos. Trans. A. Math. Phys. Eng. Sci. 366, 4205–38. doi:10.1098/rsta.2008.0111

Plank, T., 2005. Constraints from Thorium/Lanthanum on Sediment Recycling at Subduction Zones and the Evolution of the Continents 46, 921–944. doi:10.1093/petrology/egi005

Puchtel, I.S., Blichert-Toft, J., Touboul, M., Horan, M.F., Walker, R.J. 2016.The coupled ^{182}W-^{142}Nd record of early terrestrial mantle differentiation. Geochem. Geophys. Geosyst., 17, 2168-2193, doi:10.1002/2016GC006324

Qin, L., Carlson, R.W., Alexander, C.M.O., 2011. Correlated nucleosynthetic isotopic variability in Cr, Sr, Ba, Sm, Nd and Hf in Murchison and QUE 97008. Geochim. Cosmochim. Acta 75, 7806–7828. doi:10.1016/j.gca.2011.10.009

Reagan, M.K., Stern, R.J., Kelley, K.A., Bloomer, S.H., Fryer, P., Hanan, B.B., Vargas, R.H., 2010. Fore - arc basalts and subduction initiation in the Izu - Bonin - Mariana system. Geochemistry, Geophys. Geosystems 11. doi:10.1029/2009GC002871

Rizo, H., Boyet, M., Blichert-Toft, J., O'Neil, J., Rosing, M.T., Paquette, J.-L., 2012. The elusive Hadean enriched reservoir revealed by ^{142}Nd deficits in Isua Archaean rocks. Nature 491, 96–100. doi:10.1038/nature11565

Rizo, H., Boyet, M., Blichert-Toft, J., Rosing, M., 2011. Combined Nd and Hf isotope evidence for deep-seated source of Isua lavas. Earth Planet. Sci. Lett. 312, 267–279. doi:10.1016/j.epsl.2011.10.014

Robin, C.M.I., Bailey, R.C., 2009. Simultaneous generation of Archean crust and subcratonic roots by vertical tectonics. Geology 37, 523–526. doi:10.1130/G25519A.1

Roth, A.S.G., Bourdon, B., Mojzsis, S.J., Rudge, J.F., Guitreau, M., Blichert-Toft, J., 2014. Combined ^{147,146}Sm- ^{143,142}Nd constraints on the longevity and residence time of early terrestrial crust. Geochemistry, Geophys. Geosystems 15, 2329–2345. doi:10.1002/2014GC005313

Roth, A.S.G., Bourdon, B., Mojzsis, S.J., Touboul, M., Sprung, P., Guitreau, M., Blichert-Toft, J., 2013. Inherited ^{142}Nd anomalies in Eoarchean protoliths. Earth Planet. Sci. Lett. 361, 50–57. doi:10.1016/j.epsl.2012.11.023

Shirey, S.B., Richardson, S.H., 2011. Start of the Wilson Cycle at 3 Ga Shown by Diamonds from Subcontinental Mantle. Science. 333, 434–436. doi:10.1126/science.1206275

Simard, M., Parent, M., David, J., Sharma, K.N.M., 2003. Géologie de la région de la rivière Innuksuac (SNRC 34K et 34L). Ministères des Ressources Nat. Québec RG 2002–10.

Sleep, N.H., Windley, B.F., 1982. Archean Plate Tectonics: Constraints and Inferences. J. Geol. 90, 363–379. doi:10.1086/628691

Stevenson, R., David, J., Parent, M., 2006. Crustal evolution of the western Minto Block, northern Superior Province, Canada. Precambrian Res. 145, 229–242. doi:10.1016/j.precamres.2005.12.004

Taylor, S.R., McLennan, S.M., 1985. The Continental Crust: its Composition and Evolution. Oxford: Blackwell Scientific.

Touboul, M., Liu, J., O'Neil, J., Puchtel, I.S., Walker, R.J., 2014. New insights into the Hadean mantle revealed by ^{182}W and highly siderophile element abundances of supracrustal rocks from the Nuvvuagittuq Greenstone Belt, Quebec, Canada. Chem. Geol. 383, 63–75. doi:10.1016/j.chemgeo.2014.05.030

Turner, S., Rushmer, T., Reagan, M., Moyen, J.-F., 2014. Heading down early on? Start of subduction on Earth. Geology 42, 139–142. doi:10.1130/G34886.1

Van Hunen, J., van den Berg, A.P., 2008. Plate tectonics on the early Earth: Limitations imposed by strength and buoyancy of subducted lithosphere. Lithos 103, 217–235. doi:10.1016/j.lithos.2007.09.016

Van Thienen, P., van den Berg, A.P., Vlaar, N.J., 2004. Production and recycling of oceanic crust in the early Earth. Tectonophysics 386, 41–65. doi:10.1016/j.tecto.2004.04.027

Vlaar, N.J., van Keken, P.E., van den Berg, A.P., 1994. Cooling of the earth in the Archaean: Consequences of pressure-release melting in a hotter mantle. Earth Planet. Sci. Lett. 121, 1–18. doi:10.1016/0012-821X(94)90028-0

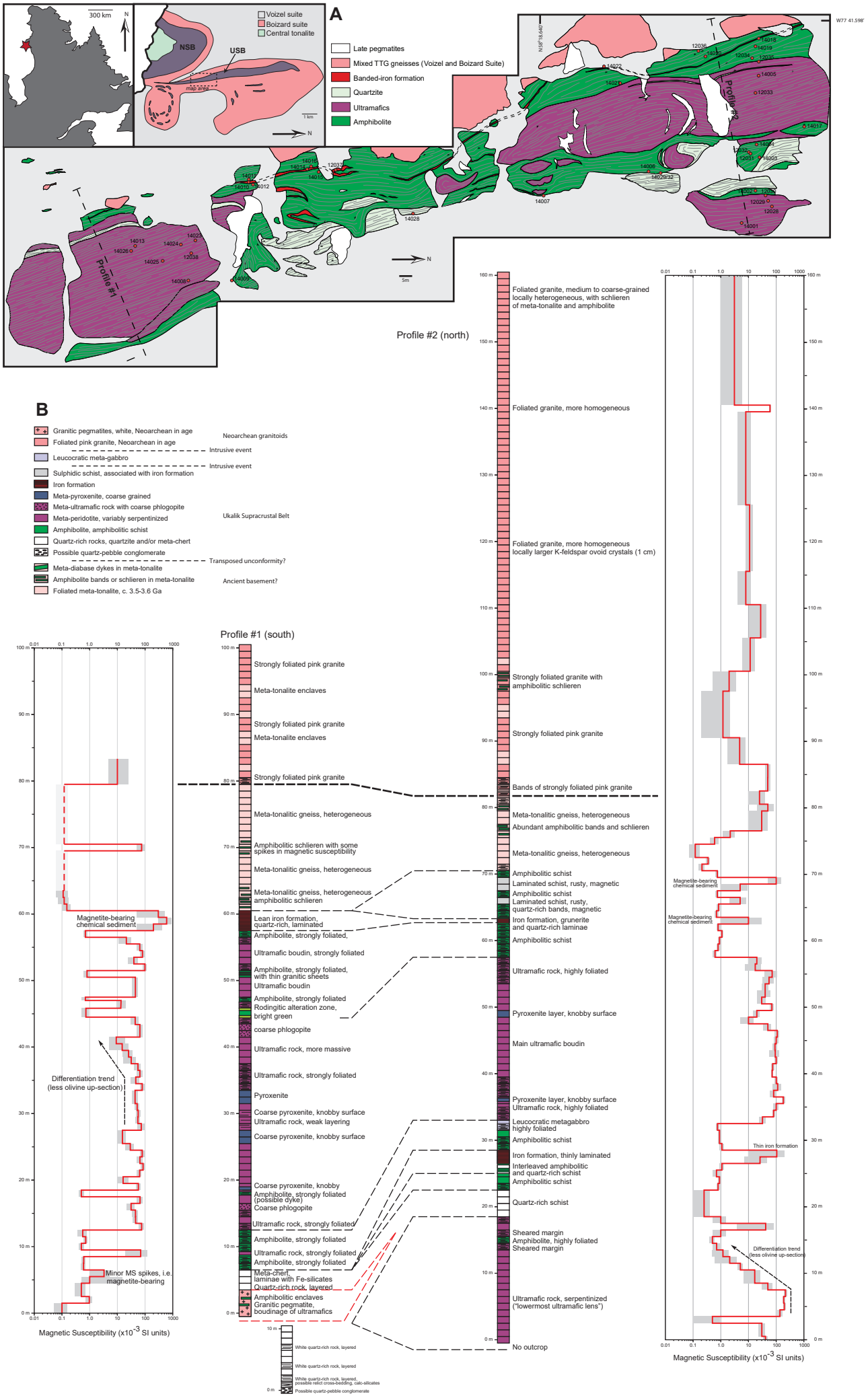
A
Voizel suite
Boizard suite
Central tonalite
NSB
USB
map area
300 km
1 km
Late pegmatites
Mixed TTG gneisses (Voizel and Boizard Suite)
Banded-iron formation
Quartzite
Ultramafics
Amphibolite
Profile #1
Profile #2
5m
B
Granitic pegmatites, white, Neoarchean in age
Foliated pink granite, Neoarchean in age
Neoarchean granitoids
Intrusive event
Leucocratic meta-gabbro
Intrusive event
Sulphidic schist, associated with iron formation
Iron formation
Meta-pyroxenite, coarse grained
Meta-ultramafic rock with coarse phlogopite
Meta-peridotite, variably serpentinized
Ukalik Supracrustal Belt
Amphibolite, amphibolitic schist
Quartz-rich rocks, quartzite and/or meta-chert
Possible quartz-pebble conglomerate
Transposed unconformity?
Meta-diabase dykes in meta-tonalite
Amphibolite bands or schlieren in meta-tonalite
Ancient basement?
Foliated meta-tonalite, c. 3.5-3.6 Ga
Profile #1 (south)
Strongly foliated pink granite
Meta-tonalite enclaves
Strongly foliated pink granite
Meta-tonalite enclaves
Strongly foliated pink granite
Meta-tonalitic gneiss, heterogeneous
Amphibolitic schlieren with some spikes in magnetic susceptibility
Meta-tonalitic gneiss, heterogeneous
Meta-tonalitic gneiss, heterogeneous amphibolitic schlieren
Lean iron formation, quartz-rich, laminated
Amphibolite, strongly foliated,
Ultramafic boudin, strongly foliated
Amphibolite, strongly foliated, with thin granitic sheets
Ultramafic boudin
Amphibolite, strongly foliated
Rodingitic alteration zone, bright green
coarse phlogopite
Ultramafic rock, more massive
Ultramafic rock, strongly foliated
Pyroxenite
Coarse pyroxenite, knobby surface
Ultramafic rock, weak layering
Coarse pyroxenite, knobby surface
Coarse pyroxenite, knobby
Amphibolite, strongly foliated (possible dyke)
Coarse phlogopite
Ultramafic rock, strongly foliated
Amphibolite, strongly foliated
Ultramafic rock, strongly foliated
Amphibolite, strongly foliated
Meta-chert, laminae with Fe-silicates
Quartz-rich rock, layered
Amphibolitic enclaves
Granitic pegmatite, boudinage of ultramafics
White quartz-rich rock, layered
White quartz-rich rock, layered
White quartz-rich rock, layered, possible relict cross-bedding, calc-silicates
Possible quartz-pebble conglomerate
Magnetite-bearing chemical sediment
Differentiation trend (less olivine up-section)
Minor MS spikes, i.e. magnetite-bearing
Magnetic Susceptibility (x10-3 SI units)
Profile #2 (north)
Foliated granite, medium to coarse-grained locally heterogeneous, with schlieren of meta-tonalite and amphibolite
Foliated granite, more homogeneous
Foliated granite, more homogeneous locally larger K-feldspar ovoid crystals (1 cm)
Strongly foliated granite with amphibolitic schlieren
Strongly foliated pink granite
Bands of strongly foliated pink granite
Meta-tonalitic gneiss, heterogeneous
Abundant amphibolitic bands and schlieren
Meta-tonalitic gneiss, heterogeneous
Amphibolitic schist
Laminated schist, rusty, magnetic
Amphibolitic schist
Laminated schist, rusty, quartz-rich bands, magnetic
Iron formation, grunerite and quartz-rich laminae
Amphibolitic schist
Ultramafic rock, highly foliated
Pyroxenite layer, knobby surface
Main ultramafic boudin
Pyroxenite layer, knobby surface
Ultramafic rock, highly foliated
Leucocratic metagabbro highly foliated
Amphibolitic schist
Iron formation, thinly laminated
Interleaved amphibolitic and quartz-rich schist
Amphibolitic schist
Quartz-rich schist
Sheared margin
Amphibolite, highly foliated
Sheared margin
Ultramafic rock, serpentinized ("lowermost ultramafic lens")
No outcrop
Magnetite-bearing chemical sediment
Magnetite-bearing chemical sediment
Thin iron formation
Differentiation trend (less olivine up-section)
Magnetic Susceptibility (x10-3 SI units)

FIGURE 2

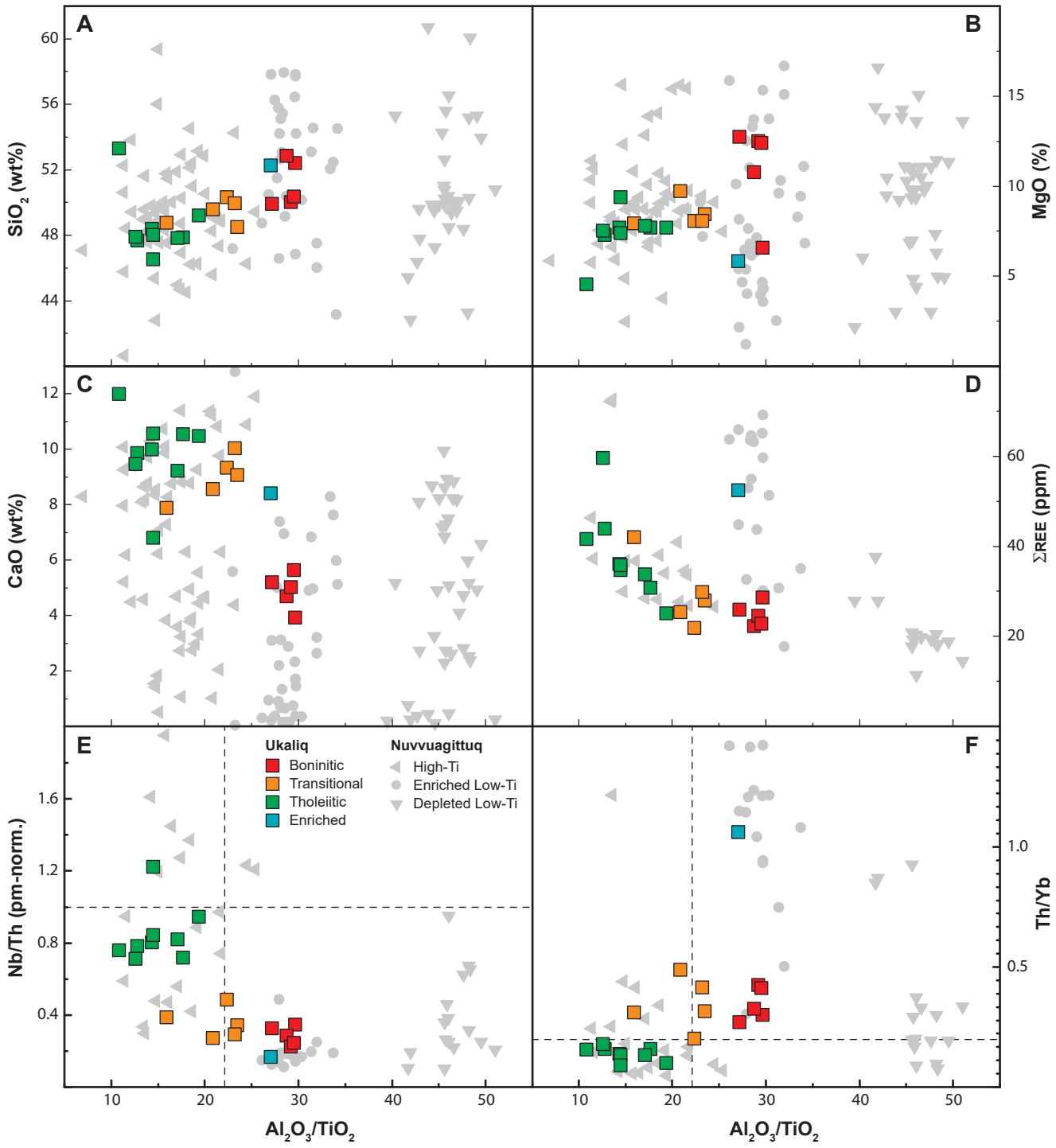
A
B
C
D
E
F
SiO2 (wt%)
MgO (%)
CaO (wt%)
ΣREE (ppm)
Nb/Th (pm-norm.)
Th/Yb
Al2O3/TiO2
Al2O3/TiO2
Ukaliq
Boninitic
Transitional
Tholeiitic
Enriched
Nuvvuagittuq
High-Ti
Enriched Low-Ti
Depleted Low-Ti

FIGURE 3

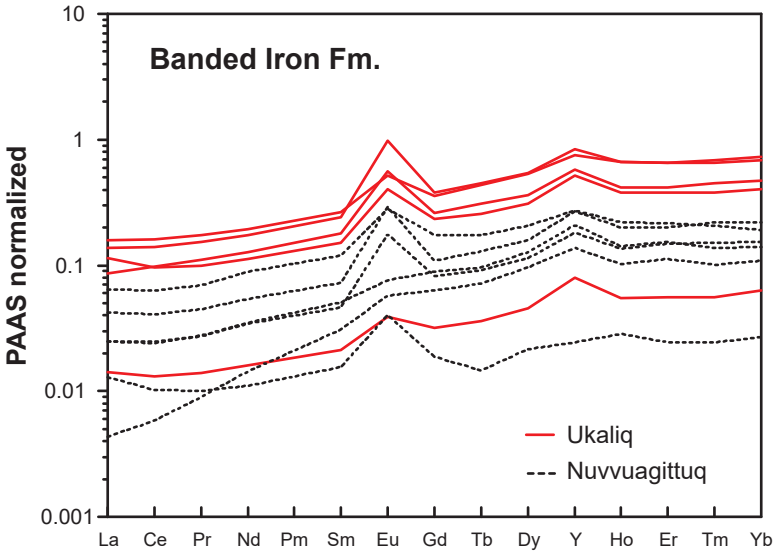
Banded Iron Fm.
PAAS normalized
10
1
0.1
0.01
0.001
La
Ce
Pr
Nd
Pm
Sm
Eu
Gd
Tb
Dy
Y
Ho
Er
Tm
Yb
Ukaliq
Nuvvuagittuq

FIGURE 4

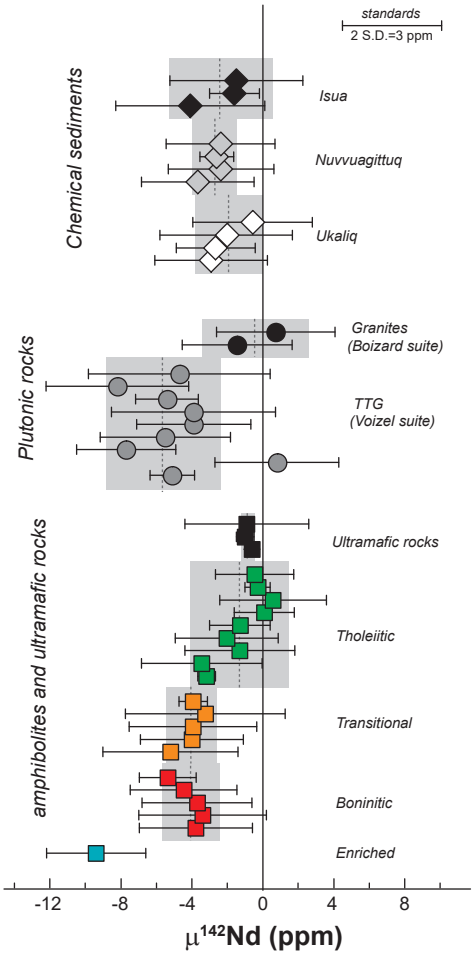
standards
2 S.D.=3 ppm
Chemical sediments
Isua
Nuvvuagittuq
Ukaliq
Plutonic rocks
Granites
(Boizard suite)
TTG
(Voizel suite)
amphibolites and ultramafic rocks
Ultramafic rocks
Tholeiitic
Transitional
Boninitic
Enriched
-12
-8
-4
0
4
8
μ142Nd (ppm)

FIGURE 5

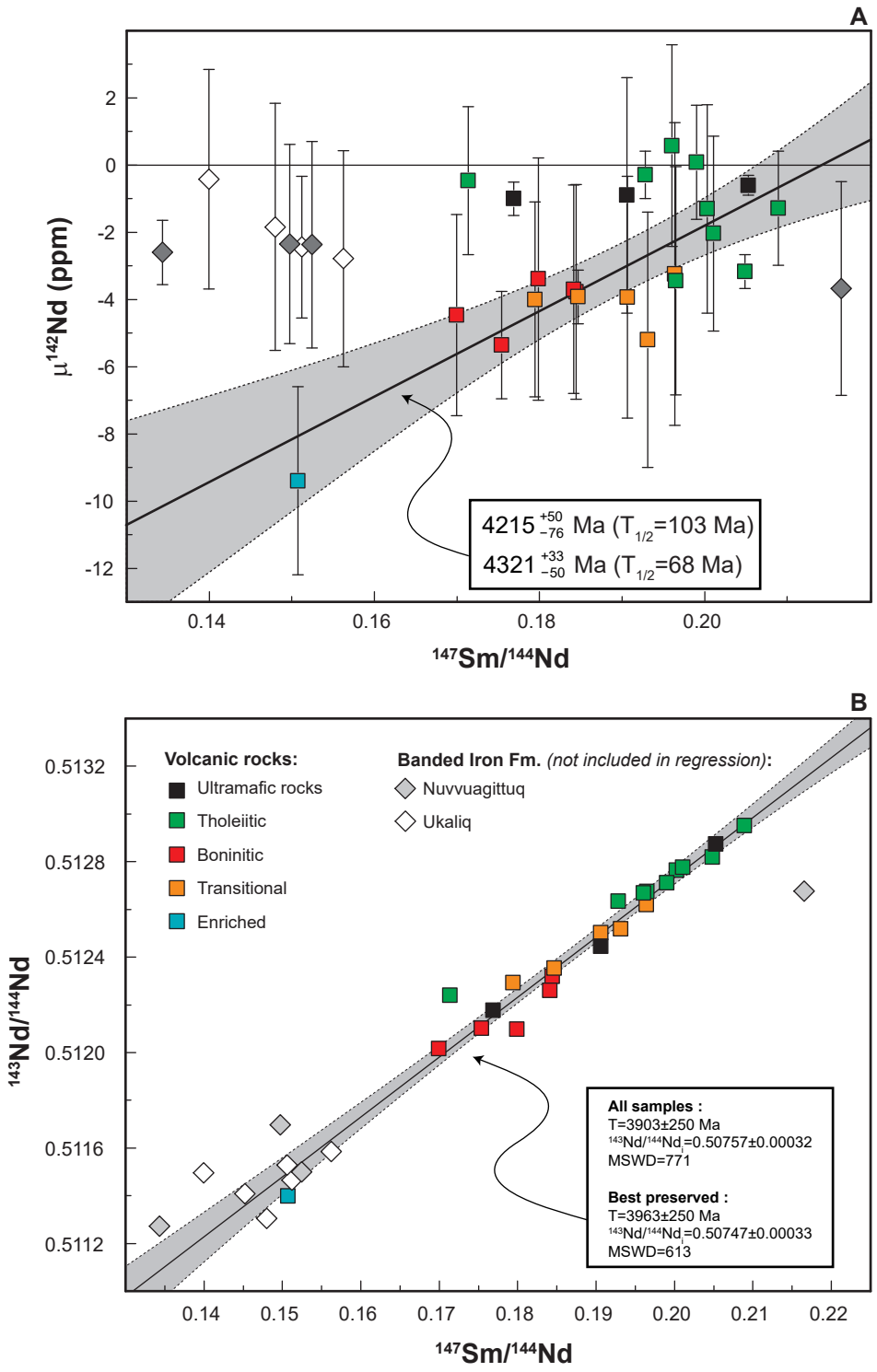
A
μ142Nd (ppm)
147Sm/144Nd
4215 +50 −76 Ma (T1/2=103 Ma)
4321 +33 −50 Ma (T1/2=68 Ma)
B
143Nd/144Nd
147Sm/144Nd
Volcanic rocks:
Ultramafic rocks
Tholeiitic
Boninitic
Transitional
Enriched
Banded Iron Fm. (not included in regression):
Nuvvuagittuq
Ukaliq
All samples :
T=3903±250 Ma
143Nd/144Nd=0.50757±0.00032
MSWD=771
Best preserved :
T=3963±250 Ma
143Nd/144Nd=0.50747±0.00033
MSWD=613

FIGURE 6

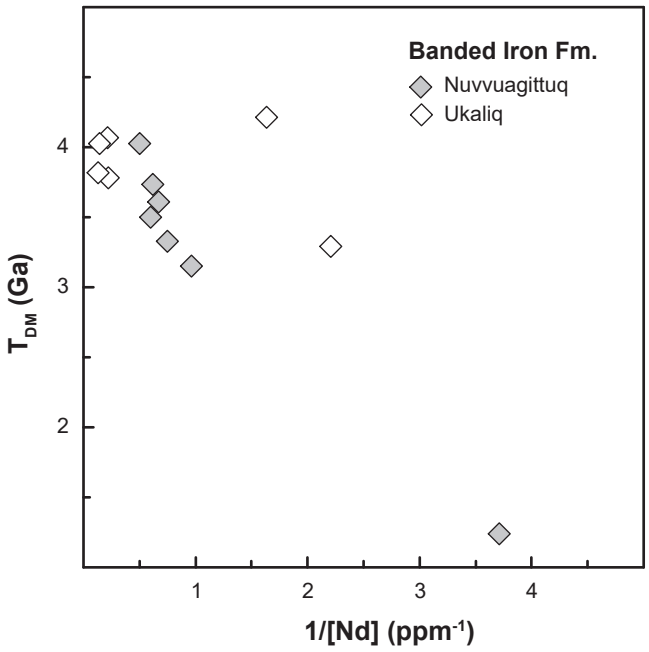

FIGURE 7

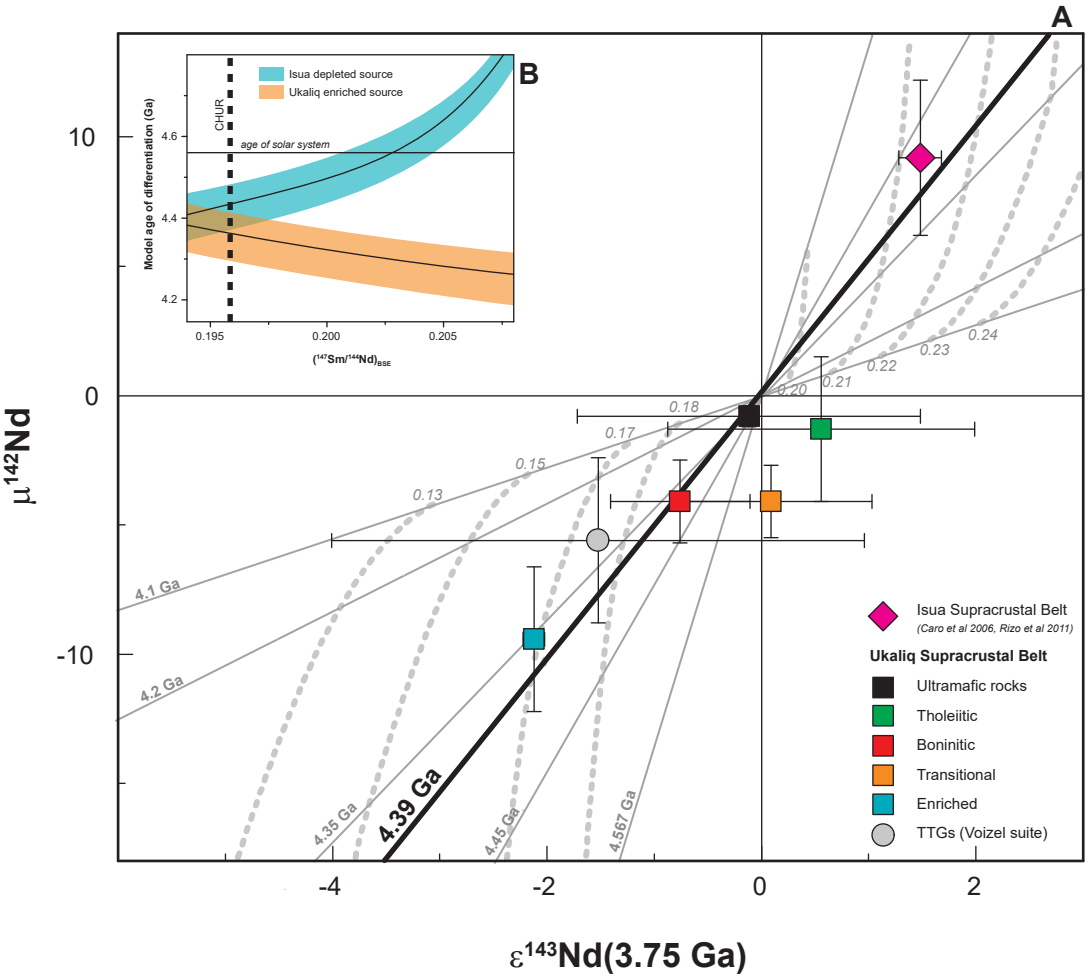
A
B
Isua depleted source
Ukaliq enriched source
CHUR
age of solar system
Model age of differentiation (Ga)
4.6
4.4
4.2
0.195
0.200
0.205
(147Sm/144Nd)BSE
10
0
-10
-4
-2
0
2
μ142Nd
ε143Nd(3.75 Ga)
0.13
0.15
0.17
0.18
0.20
0.21
0.22
0.23
0.24
4.1 Ga
4.2 Ga
4.35 Ga
4.39 Ga
4.45 Ga
4.567 Ga
Isua Supracrustal Belt
(Caro et al 2006, Rizo et al 2011)
Ukaliq Supracrustal Belt
Ultramafic rocks
Tholeiitic
Boninitic
Transitional
Enriched
TTGs (Voizel suite)

FIGURE 8

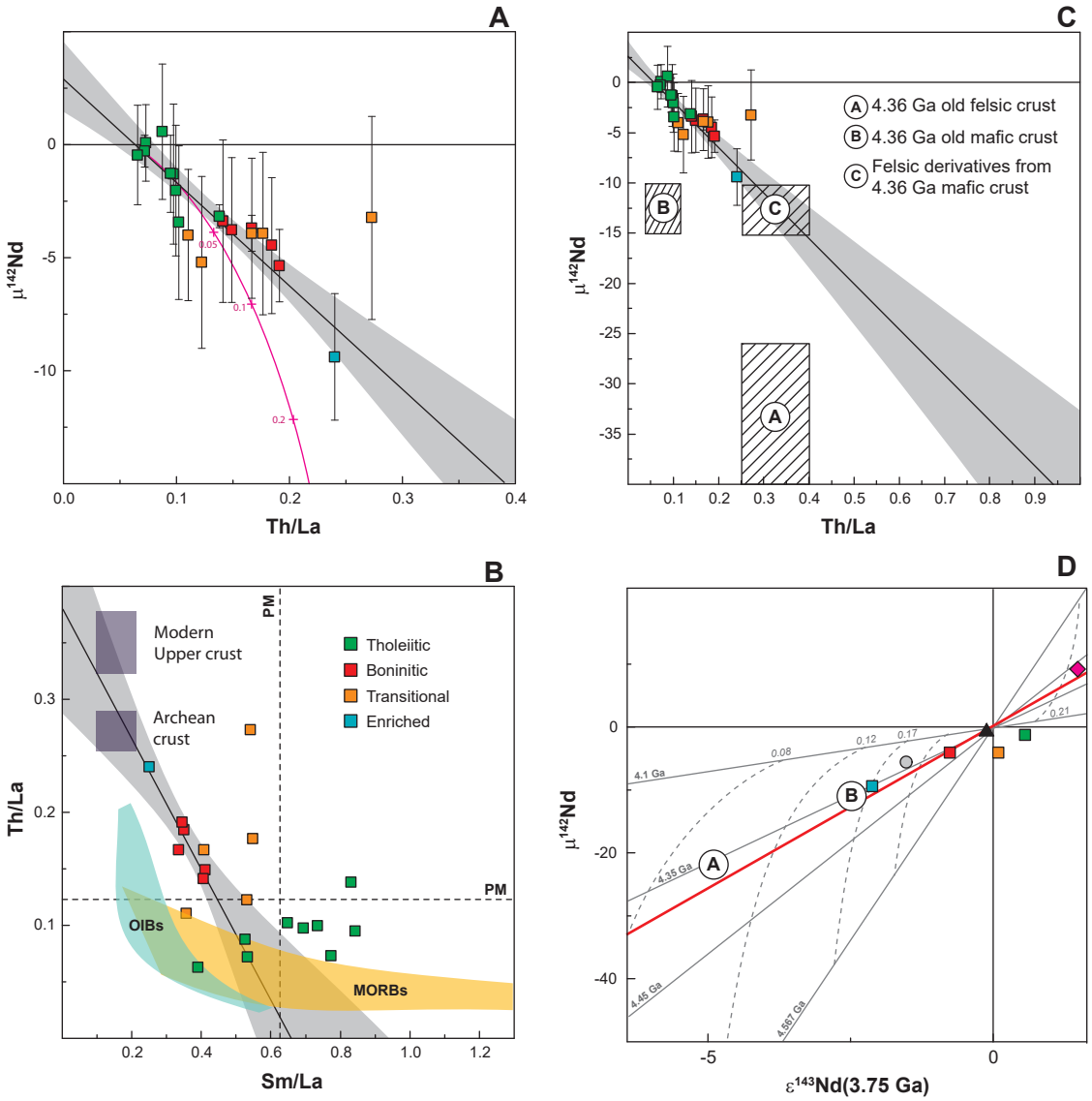
A
μ142Nd
Th/La
0.05
0.1
0.2
C
A 4.36 Ga old felsic crust
B 4.36 Ga old mafic crust
C Felsic derivatives from 4.36 Ga mafic crust
B
C
A
μ142Nd
Th/La
B
Modern Upper crust
Archean crust
Tholeiitic
Boninitic
Transitional
Enriched
PM
PM
OIBs
MORBs
Th/La
Sm/La
D
0.08
0.12
0.17
0.21
4.1 Ga
4.35 Ga
4.45 Ga
4.567 Ga
B
A
μ142Nd
ε143Nd(3.75 Ga)

FIGURE 9

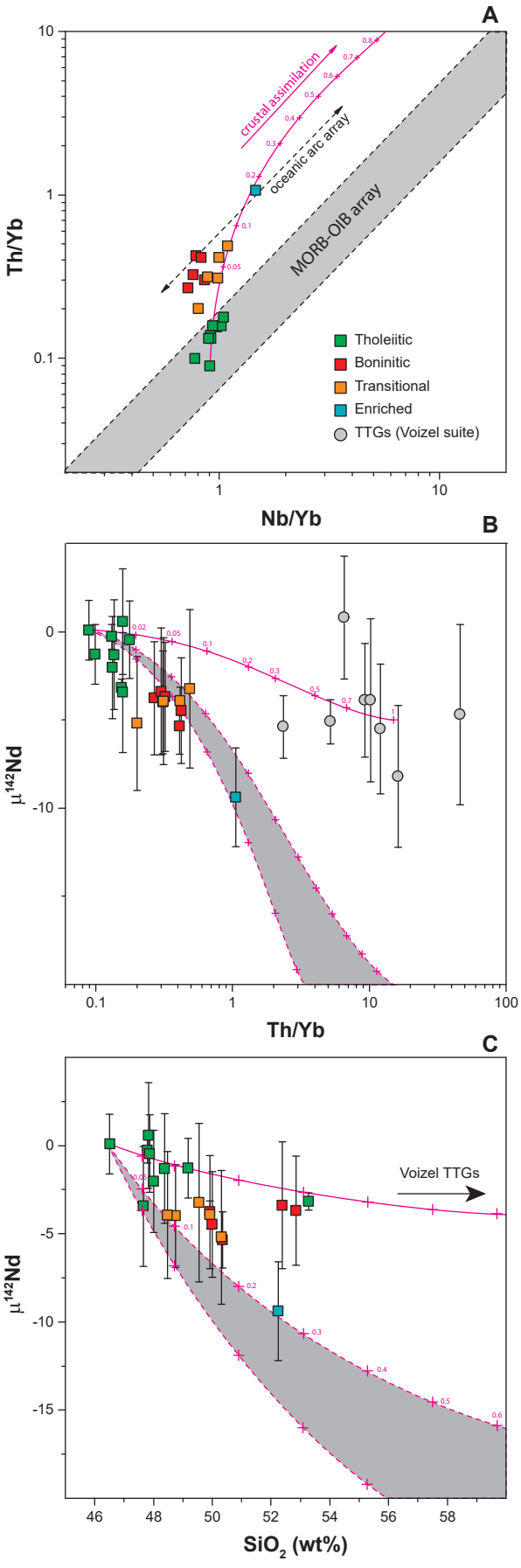
A
Th/Yb
Nb/Yb
crustal assimilation
oceanic arc array
MORB-OIB array
Tholeiitic
Boninitic
Transitional
Enriched
TTGs (Voizel suite)
B
μ142Nd
Th/Yb
C
μ142Nd
SiO2 (wt%)
Voizel TTGs

FIGURE 10

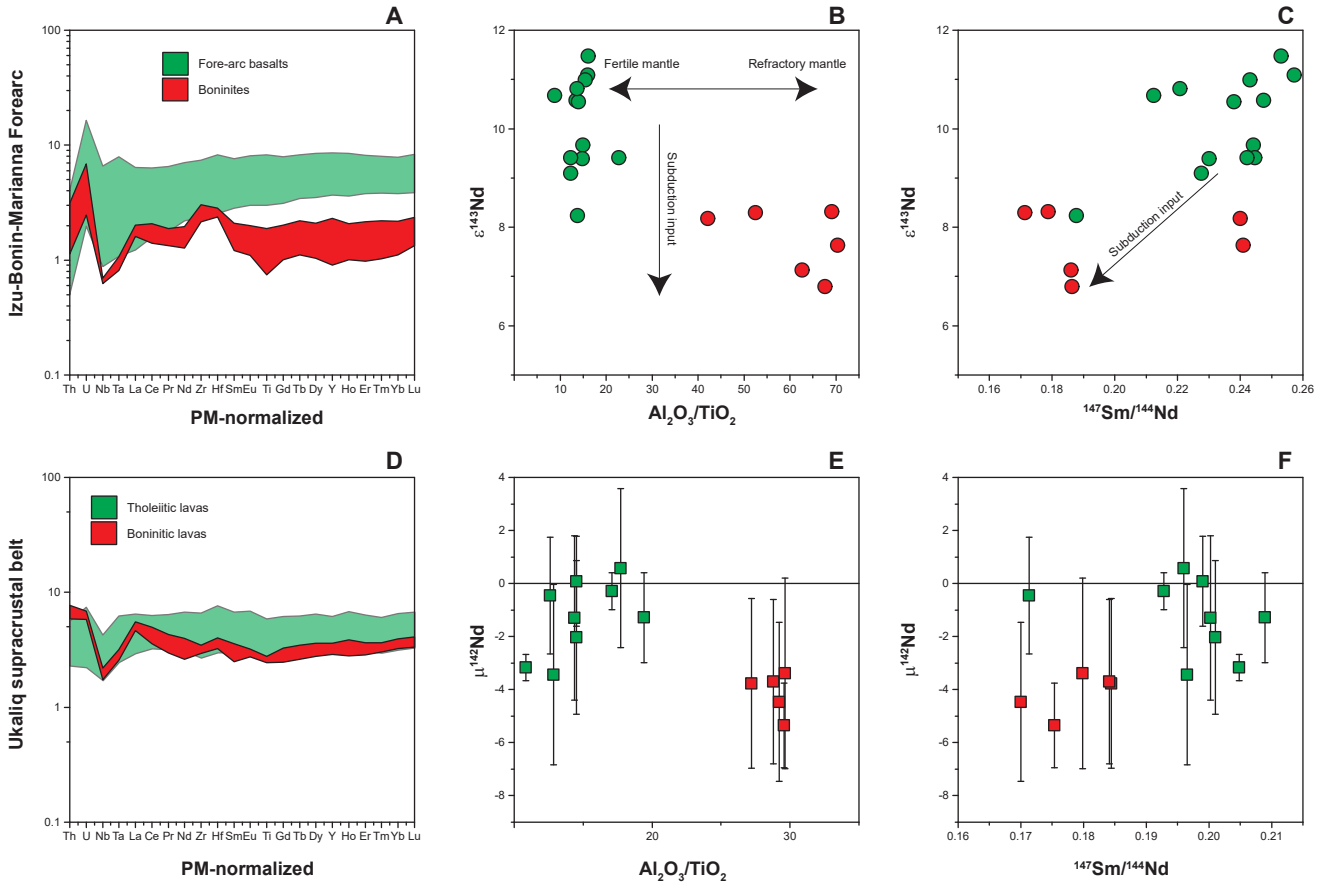
A
Izu-Bonin-Marianna Forearc
Fore-arc basalts
Boninites
PM-normalized
Th U Nb Ta La Ce Pr Nd Zr Hf Sm Eu Ti Gd Tb Dy Y Ho Er Tm Yb Lu
B
Fertile mantle
Refractory mantle
Subduction input
^{143}Nd
Al_2O_3/TiO_2
C
Subduction input
^{143}Nd
$^{147}Sm/^{144}Nd$
D
Ukaliq supracrustal belt
Tholeiitic lavas
Boninitic lavas
PM-normalized
E
$\mu^{142}Nd$
Al_2O_3/TiO_2
F
$\mu^{142}Nd$
$^{147}Sm/^{144}Nd$